FACULTY OF SCIENCE AND TECHNOLOGY

MASTER'S THESIS

Study programme / specialisation: City and Regional Planning	The *spring* semester, *2023* Open
Author: Jennifer Marie Sanders	
Supervisor at UiS: Harald N. Røstvik Co-supervisor: Hassan Gholami External supervisor(s):	
Thesis title: The Impact of Urban Context and Configuration on the Solar Energy Potential of Urban Areas	
Credits (ECTS): 30	
Keywords: solar, urban planning, city planning, building density, solar glazing, ratio, renewable energy	Pages: 78 + appendix: 10 Total: 88 Stavanger, *July 15th, 2023*

Index

Acknowledgments

I would like to thank my supervisors, professor **Harald N. Røstvik** and **Hassan Gholami** for their combined input and guidance throughout this process. On a more personal note, I would like to thank four people who are of the highest importance to me and without whom I would not have been able to complete this degree. The first is my mother, **Marie Sanders**, for her loving support and encouragement to pursue higher education, despite the difficulties encountered along the way. Furthermore, I would like to thank my fiancé, **Leon Marbl**, for helping me adjust to life in Norway and supporting me. Finally, I would like to thank my dear friends, **Simen Stormyr** and **Andrew Thompson**, for their indispensable kindness, support, and encouragement.

Introduction

The aim of this thesis is to examine the key features of city planning that impact solar potential in dense urban areas. For the purposes of this thesis, the case studies are focused on mid-rise, defined here as buildings of four to eight stories, and high-rise, defined here as buildings with nine or more stories, structures clustered together. As a variety of solar products can be combined in an assortment of configurations on most building surfaces. The projected output from these theoretical arrays can be greatly affected by the latitude of the location, the installation's direction, and surrounding shading structures.

The relevance of this focus is not that there is a gap in knowledge in this area, but rather, a lack of interdisciplinary cooperation. Planners must consider the needs of many stakeholders- property owners, city officials, neighbouring residents, construction firms, architects, and financiers, to name a few. Renewable energy systems such as solar power are grounded in the energy sector, developed by engineers and installed most often by independent companies. Although building integrated photovoltaic (BIPV) systems are considered early in the design phase, stand-alone solar systems are often treated as an afterthought, developed when a project approaches completion, or an upgrade, should the owner be strongly motivated to do invest in the technology later.

A greater adoption of renewable energy technologies has an array of benefits, which scale to the degree of the technology's application. An energy grid with multiple sources of energy generation is more adaptable; if a strain develops in one individual part of the grid, another may increase production to cover the

deficit. In this way, it is also more resilient when adapting to changing demands over time. Renewable energy systems can contribute to a country's energy security and energy sovereignty, by increasing local production and decreasing dependency on energy exchanges. Solar power is among the renewables that do not generate pollutants, such as greenhouse gasses, over the lifetime of their usage compared to traditional fossil fuel based energy sources. Although a relatively clean energy source, it is necessary to include that the mining and manufacturing of the necessary components for photovoltaic panels can be an environmentally damaging process and must be ethically sourced. If done thoughtfully, the application of solar technology can dually contribute to combating climate change and maintaining a clean environment. One notable deterrent to transitioning to renewable resources is a high initial investment. However, in the lifetime of the installation, "once a renewable energy generation system is in place, future running costs are usually very low due to an inexpensive and abundant supply of the energy source." (*Urban Energy | UN-Habitat*, n.d.). There are many policy incentives that can encourage broader adoption of renewables on an individual scale or mandates to transition to renewables on a large scale.

The full relationship between cities and the energy needed to operate them cannot lie completely outside the scope of the attention of planners when urban areas "consume 75 per cent of global primary energy and emit between 50 and 60 per cent of the world's total greenhouse gases. This figure rises to approximately 80 per cent when the indirect emissions generated by urban inhabitants are included." (*Urban Energy | UN-Habitat*, n.d.). Even when only examining existing buildings "about 35% of the EU's buildings are over 50 years

old and almost 75% of the building stock is energy inefficient. At the same time, only about 1% of the building stock is renovated each year" (*Energy Performance of Buildings Directive*, n.d.). The aim of this thesis is to present strategies for planners to examine the feasibility of large-scale solar installations as well as methods to maximize the effectiveness of these in urban areas. This serves as a point of connection partially bridging the gap between the planners and other technical disciplines in the energy sector to facilitate increasing energy production in the very areas that consume the most electricity. While this approach is aimed to contribute to net zero energy areas or even energy plus areas, rising energy demand may cause these methods to become necessary merely to maintain a steady supply.

One of the responsibilities in city planning is to remember that urban design is not limited to the experience of a single generation. Many of the current densest cities have been continuously inhabited by humans for hundreds or even thousands of years, evolving over time. With the expectation of this progresses, planners must acknowledge and respect the heritage of an area while also understanding that the new developments that are planned, designed, and built will far outlive the individuals behind their construction. The development of cities goes on shape experiences of people for generations after the projects are completed. Urban planners must anticipate and adapt to design with new technological innovations in mind or developments may fail to meet the needs of future residents.

Through a series of evaluations and calculations, this thesis has prepared a set of recommendations for maximising the solar potential of installations as well as showcasing the potential of the integration of these technologies in the built

environment. These recommendations may serve as a set of guidelines in new construction as well as retrofitting existing buildings to serve a portion of a city's energy needs through solar installations.

Research Aims

The aim of this thesis is to simplify buildings of similar morphological styles used in urban planning based on the factors of street grid rotation, building height, intermittent spacing between buildings, and angle of sunlight for a given season to determine the solar potential of a given area. Literary research is applied to examinations of relevant regulations that could influence the potential implementation large scale solar developments in urban areas. Limited case studies of existing building areas in densities of mid-rise and high-rise construction investigate the impact these factors have on the solar energy potential of building skins. The goal was to develop a simplified method of calculating approximate solar potential for building skins that can be applied over an area of multiple city blocks using the location’s latitude, street grid rotation, average height, and average street width. The purpose of these findings is to showcase the possible applications of planning strategies for transforming existing districts and building new districts into nearly zero energy or energy positive areas with solar installations.

Methodology

The literature analysis examines relevant scholarly sources with information pertaining to the policies influencing solar installations and components that factor into the calculations. Later chapters apply a series of calculations to give additional context to the application of these theoretical solar installations. These are compiled in a matrix in Microsoft Excel for side-by-side comparison and ease of alteration with the sets of calculations instantaneously updated when variables are changed. In simplest terms, the calculations are used to combine the area and solar irradiance as shown in the equation below with the units for these calculations. Standard values for the efficiency of the system are used based on the performance of solar products and the percent of façade used is based on an estimated façade evaluation for features such as downspouts, ornamental window trim, pilasters, and other façade features which vertical solar installations must be installed around. Solar irradiation is standardly measured in kilowatt hours, though the more appropriate unit of megawatt hours is used for final values of solar production to better convey the quantity of energy for this scale.

$$Solar\ Irradiation\ \left(\frac{kwh}{m^2}\right) \times Area\ of\ Installation\ (m^2)$$
$$\times Efficiency\ of\ System \times Percent\ of\ Facade\ Used$$
$$= Solar\ Production\ (kwh)$$
$$\frac{kilowatt\ hours\ (kwh)}{1000} = Megawatt\ hours\ (Mwh)$$

When the scale of installations spans multiple city blocks, determining the area of solar installations involves many steps before accounting for additional factors, such as shading. For case studies and example calculations, it is

necessary to have cite specific information about the location. Using the tool plugin for “open street maps” for the program QGIS for producing accurate building footprints, which are then imported into AutoCAD to separate into different directional components. Generally, the optimal solar directions in the northern hemisphere are south facing and in the southern hemisphere is north facing due to the Earth’s axial tilt as it rotates. As the case studies in this thesis are all located in the northern hemisphere, the building lengths are totalled along the more relevant south-eastern, and south-western faces of the building while the remaining faces are disregarded.

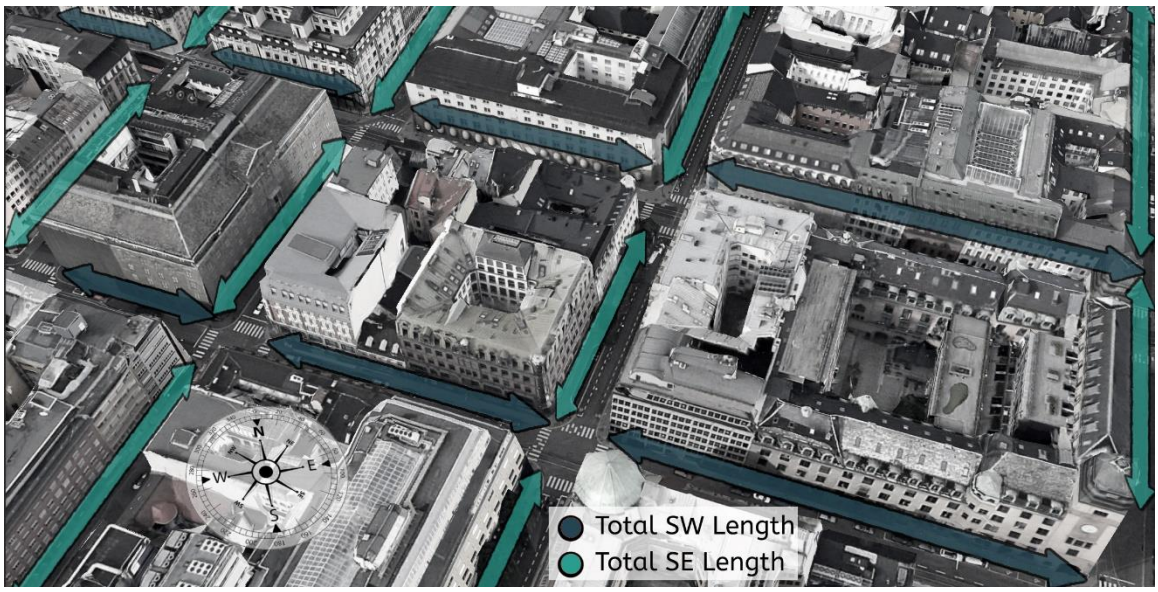

Figure 1 Total SW and SE Lengths

$$SW Length1 + SW\ Length2 \ldots = Total\ SW\ Length$$

$$SE\ Length1 + SE\ Length2 \ldots = Total\ SE\ Length$$

$$(Total\ SW\ Length\ +\ Total\ SE\ Length)\ \times\ Average\ Height\ =\ Facade\ Area$$

For the more detailed case studies are located Norway, the building heights are measured using høydedata.no, as it is a publicly accessible database of building elevation information. Other case studies use a given height to simplify

calculations. Each measured point of significant height difference from the individual buildings is input of a function of that building's footprint area proportional to the overall area of the site to find an accurate average height. For blocks with less easily decerned separation, the same process was applied by measuring the building's height at each of the south, southwestern, and southeastern corners. Each height is then multiplied by one third its area (as there are three points of measurement on each block) to make the end value proportional to area of the block. For buildings subdivided by individual height changes, these are only multiplied by the percent of the area of the subdivided compared to the total building area. This factor weighs the height of larger buildings heavier than smaller buildings to gain a more accurate height measurement. Finally, a standard of four meters is subtracted from the vertical component to remove the street level from consideration for solar applications in calculations using the adjusted average height.

$$Area1 + Area2 + Area3 = Footprint\ Area\ Total$$

$$(h1\times(Area1\div3) \div Area\ Total) + (h2\times(Area1\div3) \div Footprint\ Area\ Total) + (h3\times(Area1\div3) \div Area\ Total) + (h4\times(Area2\div3) \div Footprint\ Area\ Total) + (h5\times(Area2\div3) \div Area\ Total) + (h6\times(Area2\div3) \div Footprint\ Area\ Total) + (h7\times(Area3\div3) \div Footprint\ Area\ Total) + (h8\times(Area3\div Footprint\ Area\ Total) + (h9\times(Area3\div3) \div Footprint\ Area\ Total) = Average\ Height\ or\ Height\ Building\ (H_b)$$

$$Building\ Height\ (H_b) - 4m = Adjusted\ Average\ Height\ or\ Height\ Potential\ (H_p)$$

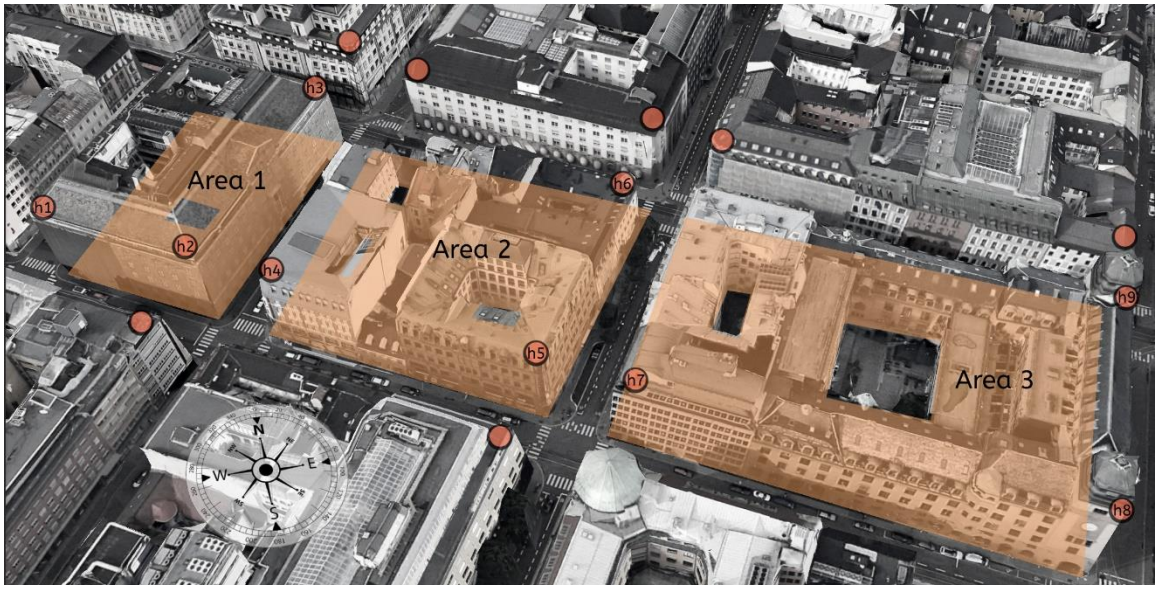

Figure 2 Averaging Heights

Once the overall dimensions of the façade are established, the area is simply the product of the height multiplied by the total southwest or total southeast length. The diagram below shows the different factors of a façade's area. The total height and width of the building are H_b and W_b, respectively. As an active street level serves many functions beyond energy generation, a standard height of four meters is subtracted from relevant calculations to remove the street level (H_s) from relevant calculations. Once the potential area is determined, only a fraction of the remaining area is a surface suitable for solar installations. Large portions of vertical façades are likewise unavailable for solar panels, due to the presence of windows, balconies, shading structures, and other similar features. To account for these suboptimal areas, only a limited percentage of each area is used. While more precise calculations can be determined with a detailed façade analysis, an approximate value is sufficient for the scope of this evaluation. The exact value depends on an analysis of the façade, though a rough approximation can be applied. In the diagram below,

the blue areas represent solar installations occupying ten percent (10%) of the potential area (green).

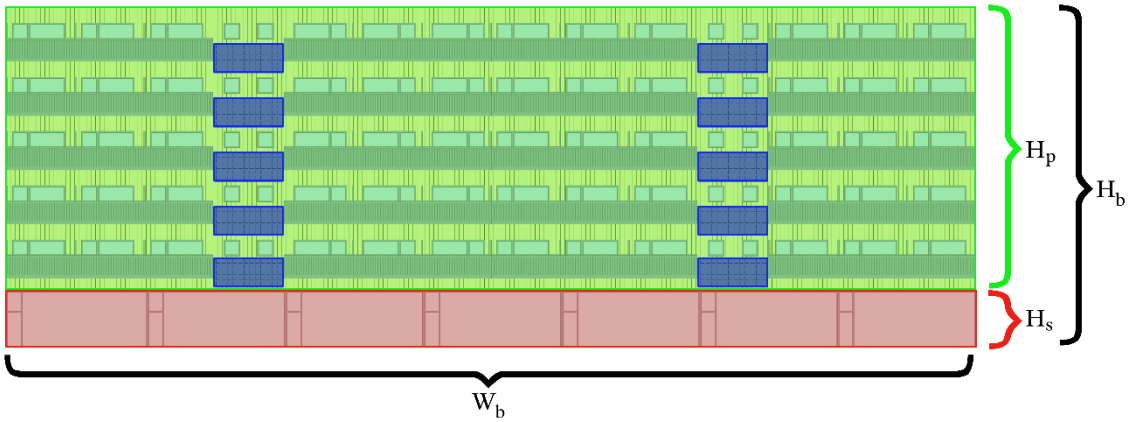

Figure 3: Terms for Facade Area

Adjusted Average Height or Height Potential (H_p) x Building Width (W_b) x Percent of Façade Available for Vertical Solar = Façade Building Area

To factor in shading, the potential height (H_p) is reduced to only the amount of the façade in direct sunlight, measured down from the top of the building. Throughout the annual revolution of the year, the sun's angle is at its lowest on the winter solstice and at the highest angle at the summer solstice, although, for further clarification, the summer solstice in the northern hemisphere occurs in June and in the southern hemisphere it occurs in December. The solar altitude angle, measured up from a horizontal plane relative to earth, at these key points of the year are used as constants for a given latitude to calculate how much sunlight may strike a vertical surface given the surrounding structures that cast shade. The method of calculating solar altitude angle at these points can be found in Table 1. AutoCAD is also used to measure street widths exported from GIS. These are combined with elements of trigonometry

to calculate the height of shadows on an adjacent surface, as shown in the figure below.

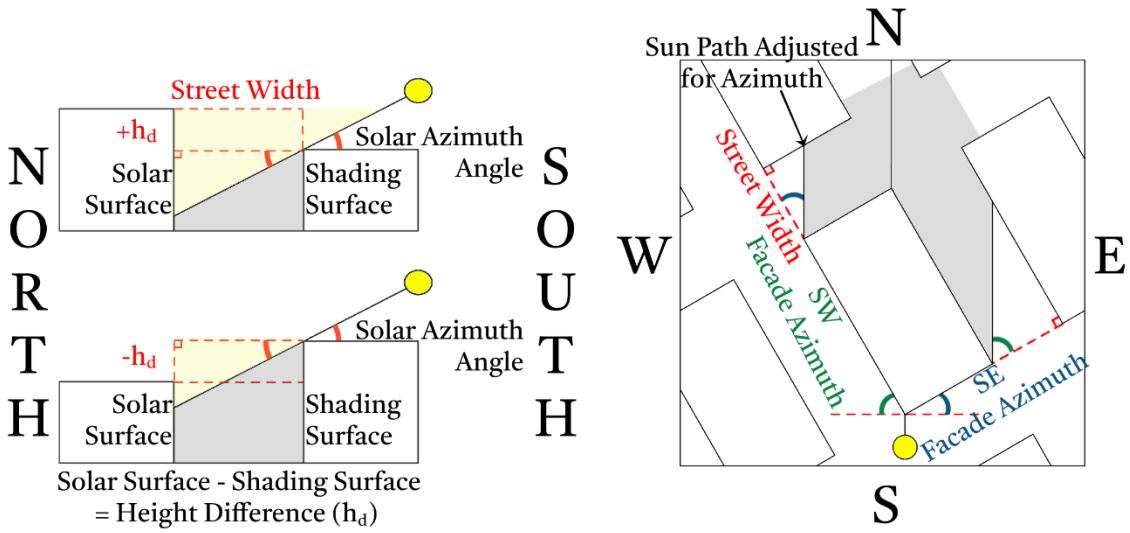

Figure 4: Shadow Trigonometry

For orthogonal areas with shadows directed due north (for northern hemisphere):

Building height in direct sunlight (measured from top of building) =

(Street Width x Tan(Solar Azimuth Angle)) + Height Difference

$$Height\ in\ direct\ sunlight = (W_s * Tan(E_w)) + h_d$$

To adjust for building azimuth:

Width adjusted for building azimuth = Street Width / (Cos(Rotation Angle)

$$W_z = W_s / (Cos(z)$$

Combined Equation:

Building height in direct sunlight (measured from top of building) =

((Street Width / Cos(Rotation Angle)) Tan(Solar Azimuth Angle))*

+ Height Difference

$$Height\ in\ direct\ sunlight = ((W_s / Cos(z)) \times Tan(\alpha)) + h_d$$

To properly account for shading and different values of solar irradiation on two building faces, these calculations must account for the different conditions. This is broken down even further when solar systems of different efficiency are used, but this is just a further extension of the following equation. This equation assumes the entire building height, though adjusted for area of installation, is converted into solar applications. However, replacing the average building height for the height of the surface in direct sunlight will result in the energy production of solar installations limited to the area of building in direct sunlight during different points in the year. The resulting area of solar installations can also be compared as a percentage of the total façade area.

$$((\text{Solar Irradiation SW } (kwh/m^2) \times \text{Total SW length } (m) \times \text{Average Building Height } (m)) + (\text{Solar Irradiation SE } (kwh/m^2) \times \text{Total SE length } (m) \times \text{Average Building Height } (m))) \times \text{Efficiency of System} \times \text{Percent of Facade Used} = \text{Solar Production } (kwh)$$

The solar irradiation for the case studies uses the online database “Photovoltaic Geographical Information Systems” to measure solar irradiation at specific locations as well as factoring in the azimuth, or rotation of the prospective installation based on the direction of the streets. Finally, all terms and values used in the calculations are defined in Table 1 below.

Table 1: Definition of Terms

	Degree of Elevation	α = Solar Altitude Angle	
Solar Altitude Summer Solstice	E_s	Solar Altitude Summer Solstice	90-Latitude+23.5 = E_s
Solar Altitude Winter Solstice	E_w	Solar Altitude Winter Solstice	90-Latitude-23.5 = E_w
Solar Altitude on Equinox	E_e	Solar Altitude on Equinox	90-Latitude = E_e

	Widths	z = Building Azimuth
Width of Street (distance between buildings assuming building azimuth (z) is 0)	W_s	Building azimuth denotes the rotation of the shape from the orthogonal, southward direction. Negative values are southeast oriented up to -90°, which is due East. Positve values are southwest oriented up to 90° is due West. 0° is oriented due South.
Width of Building (S, SE, or SW bulding length)	W_b	
Street width adjusted for building azimuth (z)	W_z	

	Area	h_d = Height Difference
Area Total	$h_b * w_b = a_b$	Height Difference is measured with the Solar Surface Building height - Shading Building height. Ex: South facing facade height - North facing facade height in the Northern Hemisphere. If solar surface<shading surface, h_d is negative.
Area Potential	$h_p * w_b = a_p$	
Area of Facade (percent of facade wish to use)	a_f	
Final Adjusted Area Accounting for Facade	$a_p * a_f = a_a$	
*Area of Facade Ex: To use 30% of the facade, $a_f = 0.3$		*Height measured down from top of south facing facade

	Building Height	W_z = Adjusted for Building Azimuth	$W_z = W_s / (Cos(z)$
Height Building Total	h_b	For these calculations, use the azimuth or rotation for the corrisponding face of the building. Eg: Southeast face = -z	
Street Height (Pedestrian Way)	(4 meters) h_s		
Height Potential	$h_t - h_s = h_p$	All calculations use Solar Noon, when Solar Azimuth is 0.	
Height Difference (between two structures)	h_d		
Height Solar Constant (always in sun/at Winter Solstice)	h_{sc}	$h_{sc} = (W_z * Tan(E_w)) + h_d$	or $h_{sc} = ((W_s / Cos(z)) * Tan(E_w)) + h_d$
Height Solar Maximum (at Summer Solstice)	h_{sm}	$h_{sm} = (W_z * Tan(E_s)) + h_d$	or $h_{sm} = ((W_s / Cos(z)) * Tan(E_s)) + h_d$
Height Solar Equinox (in sun for half of year/at Equinox)	h_e	$h_e = (W_z * Tan(E_e)) + h_d$	or $h_e = (W_s / Cos(z) * Tan(E_e)) + h_d$

Chapter 1: Types of Solar Installations

Although many renewable energy systems are limited by location to some extent, there are such a wide variety of solar products available that installations can take just as broad of a variety of forms. With the right application, just about any type of surface can be converted into a solar surface, as shown in the diagram below. Further advancements compound the flexibility of the technology, such as thin films or foils acting as solar cells with some amount of transparency, contribute to solar glazing options. Overall, the rapid advancement in solar technology has paved the way for a wide variety of applications beyond traditional rooftop solar panels. Solar technology is already reshaping many industries with innovative uses in various sectors that impact the built environment, from building integrated photovoltaic panels that act as insulated building envelop, glazing solar solutions, applications in agricultural practices, converting bodies of water into renewable energy sources, and even as art. On a smaller scale, many areas with public lighting, such as street lights or lampposts commonly charge with solar energy during the day to illuminate the night. Although there are many valid limitations to consider with this technology, a shortage of available surface area is unlikely to be the primary among them.

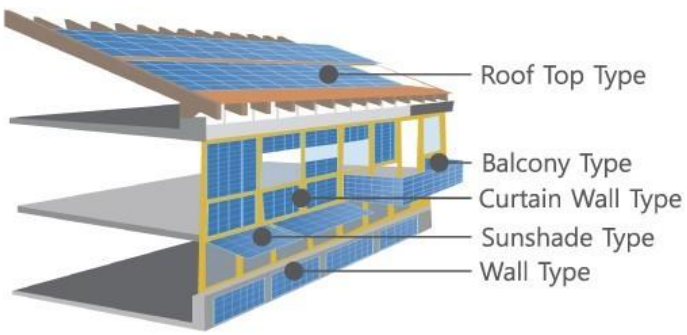

Figure 5: Variety of Installations

From the standpoint of optimizing land use for high density, traditional solar farms are wasteful, devoting a large land area to a single purpose. The United States Department of Energy projects estimates that the ground based solar

land use required to meet growing energy needs while transitioning to a carbon emission free energy grid will reach 0.5% of the contiguous U.S. surface area by 2050 (Solar Futures Study, n.d.). For comparison, urban land area is estimated to occupy “106,386 square miles, or 3% of total land area in the U.S., and is projected to more than double by 2060.” (U.S. Cities Factsheet, n.d.). If every country were to take a similar approach, this substantial area would require the development of massive swaths of natural landscapes. For the preservation of these areas as well as limiting the encroachment of developed areas on the natural environment, it is more spatially advantageous to combine the function of solar farms in urban areas that have already been developed, as both functions can coexist in the same place.

A study conducted by the Fraunhofer Institute for Solar Energy Systems examining 28 different subcategories of commercial solar modules found that the most efficient are those made from mono-crystalline silicon (NREL, 2020). The resulting efficiency of 24.4% was achieved in laboratory conditions (NREL, 2020). However, these same modules deployed in real-world conditions encounter various factors including the temperature fluctuation, snow cover, and cloud cover, which can reduce the overall efficiency of photovoltaic (PV) systems. Consequently, the average efficiency range for mono-crystalline PV systems currently available in the market is estimated to be between 15% and 20% (NREL, 2020). As a result, this range of efficiency is applied to standard panels in the case studies in later chapters.

To envision the possible applications, it is first necessary to acknowledge the wide verity of solar products available for constructing large scale solar arrays. These, combined with a corresponding energy storage system (ESS)

ensure that excess energy is stored until it is needed. For the purposes of these calculations, there are four primary systems of mounting that will be used: slopped roof mounting, flat roof mounting, vertical panel mounting, and solar glazing. Further example categories of this technology include Building Integrated Photovoltaics (BIPV), artistic solar, combined land use solutions.

Sloped Roof

Many related factors may supersede solar efficiency when considering a building's roof design, such as aesthetic preference or environmental factors. One notable example of such conditions is that steeply pitched roofs are advantageous in reducing excessive snow build up. This roof type is common for low rise, suburban areas, such as single-family housing units, and frequently in mid-rise areas. Whether the roof is a gable, hipped, single slope, or other angled arrangement- the angle should be close to that of the location's latitude while also being directed towards the optimal solar direction to maximize solar output. This direction is south facing for the northern hemisphere and north facing for the southern hemisphere. Due to the limitations of the roof configuration, only a fraction of the roof could be facing the right direction and, depending on the building's design, the angle may not match the location's latitude. Either factor has the potential to reduce the useful roof solar area or the efficiency of roof mounted panels at less than optimal direction or angle.

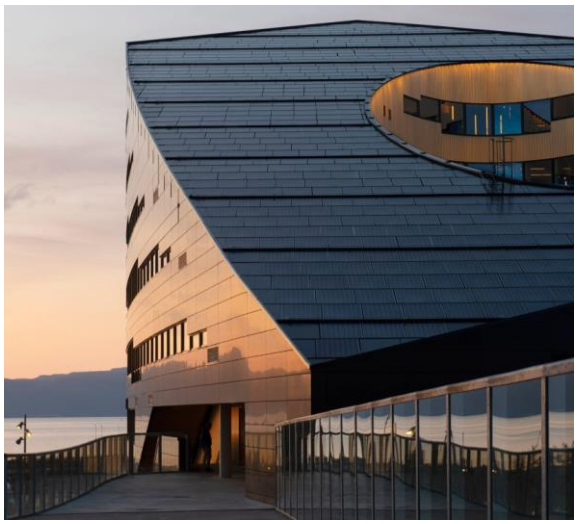

Figure 6: Powerhouse Brattørkaia, Norway

Unfortunately, due to the high variation of direction and slope in the case study areas, the impact of solar panels on sloping roofs was ommited from the calculations.

Flat Roof

Regardless of the direction the building faces or the angle of the street rotation, a flat roof has the most flexibility for setting up solar arrays at the optimal direction and angle, yielding the highest energy output of these four options. As mentioned in the sloped roof comparison, this may not always be optimal for addressing the environmental factors of the building or the overall design intentions. Likewise, for applying new solar installations to existing structures, converting an existing sloped roof into a flat roof is not among the recommendations in this thesis. Although it may be a feasible option in rare cases, the complicating factors far outweigh the possible net gain in the majority of situations.

Vertical Panels

Standard panels designed to be mounted on vertical surfaces come in a variety of designs and styles. Out of all four options, this is the only one that is publicly visible. Therefore, as the array’s visibility has an impact on the urban experience of its area, it is necessary to consider, to some extent, the aesthetic appeal of the installation. These panels are not at the optimal angle, but they do have the flexibility to be installed along the sides of the building facing the proper direction. For cases when a given roof area is not suitable or sufficient

for solar installations, a building's vertical area can be the next highest energy output alternative.

Figure 8: 550 Spencer, Australia

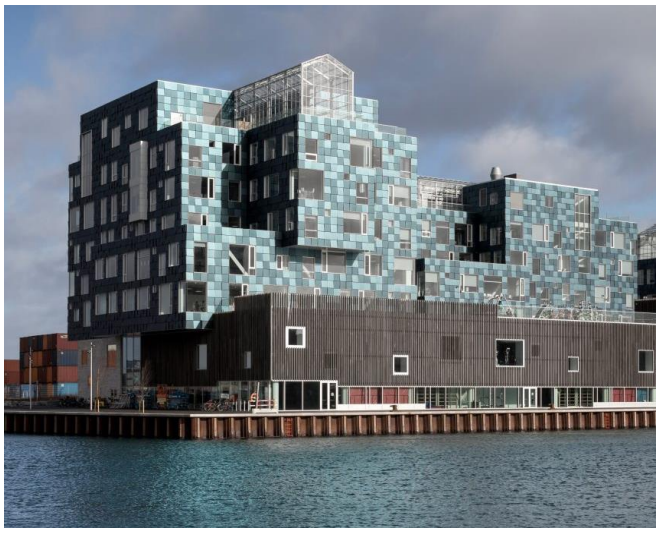

Figure 7: Copenhagen International School for Nordhavn, Denmark

Solar Glazing

This innovative solution has been developed for transparent or semi-transparent solar panels that double as window panes. Although these pose a potential renewable energy source suited for glass and steel skyscrapers, unfortunately, these typically operate at around half of the efficiency of standard panels. Currently, the efficiency of these panels is around 7% (How It Works - ClearVue PV, 2022) which is applied to the case studies in later chapters. Combining this disadvantage with the mounting angle, given that vertical installations are not the most optimal angle,

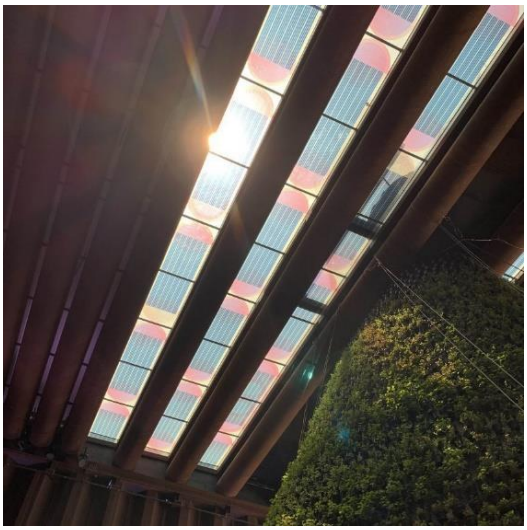

Figure 9: The Dutch Biotope, UAE

further reduces the solar capacity for this option. Another disadvantage of their construction is that although glass can be shaped and curved in a variety of ways, the construction of solar windows at their current stage of development is not necessarily equivalent.

Building Integrated Photovoltaics (BIPV)

Building Integrated Photovoltaics (BIPV) refer to the integration of solar panels directly into the building envelope, such as roofs, facades, and windows, seamlessly blending with the architectural design. Unlike traditional solar panels, which are typically added onto an existing structure, BIPV systems are designed to replace conventional building envelopes, simultaneously generating renewable energy and tethered to the structural and insulation needs of the building. This integration of solar technology into the building itself is what sets BIPV apart from standard solar panels. These are created in a variety of colors and textures, which improve the aesthetic appearance of the system, but may simultaneously negatively impact the efficiency of the system due to increased reflection or decreased absorption. The extent of the aesthetic to efficiency trade off will be determined by stakeholders associated with the earlier design phases.

The case studies in later chapters do not infer the proposed installation is composed of BIPV systems, though this is possible should the replacement be more advantageous than maintaining the existing facade. However, this is an option for new developments, as the technology becomes more affordable and accessible over time.

Artistic Solar

Beyond the technological applications, there are efforts to making these arrays of mechanical equipment visually appealing by integrating solar technology into artistic forms. Artists and designers are increasingly incorporating solar panels and solar-powered elements into their artwork that not only serve as aesthetically pleasing structures, supply clean energy, and raise awareness about sustainability. This is the goal of the various exhibits The Solar Biennale and similar events. As showcased by the examples below, the geometric forms of these arrays developed by engineers and architects can become the key design feature of a structure. The versatility of forms that solar systems can take creates the potential to blend technological innovation with artistic expression.

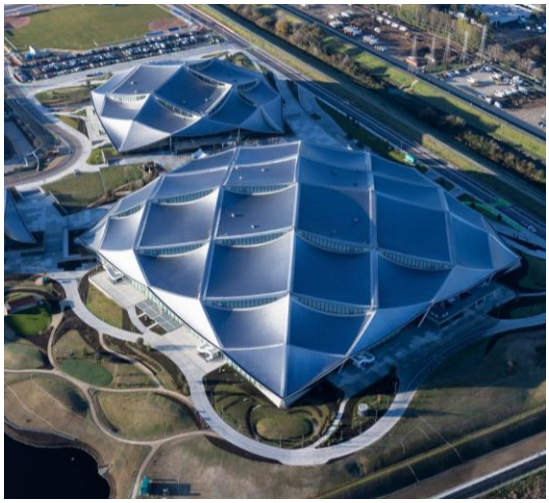

Figure 10: Bay View, USA

Figure 11: La Seine Musical, France

Figure 12: LAD headquarters, China

Combined Land Use Solutions

While not an application that explored in this thesis, it is worthy to note that this technology has expanded to the agricultural environment as well as the urban. Recent explorations into solar have the potential to change modern methods of food production as well as water collection.

Agrovoltaics is one name for the combination of agricultural land with photovoltaic panels to produce both food and energy. Depending on the climate and plant, intermittent coverage from a canopy of solar arrays can protect plants from high winds, prevent the plants from drying out through transporation when exposed to excessive sunlight, lower water loss through evaporation, and other similar benefits.

Floatovoltaics is a name for the combination of solar installations over waterways. Solar panels operate at the highest efficiency within a specific temperature range. This efficiency drops continuously at higher temperatures. Installing solar arrays over manmade waterways such as aqueducts, canals, and reservoirs can simultaneously shade the waterways to reduce evaporation while also passively cooling the panels. This has been tested with some success as a potential solution for drought ridden areas.

Chapter 2: Policy Motivations

Installation of solar applications have expanded in recent years due to the numerous environmental, economic, and social benefits. Policymakers implement a range of initiatives aimed to incentivize, promote, and regulate the use of solar energy as entities transition away from fossil fuels establish how these will feed into the established energy grid. “Both tailored policies and comprehensive policies addressing innovation systems have helped overcome the distributional, environmental and social impacts potentially associated with global diffusion of low-emission technologies.” (*IPCC, 2022: Summary for Policymakers*, p.13, H.-O. Pörtner et al. 2022). These initiatives span across various levels of government, from local municipalities to national and international bodies. The following describes a variety of incentives that promote the integration of solar systems into the existing grid.

In its chapter on cities, the most recent IPCC report states with high confidence that “in all cities and urban areas, the risk faced by people and assets from hazards associated with climate change has increased” (*Climate Change 2022: Impacts, Adaptation, and Vulnerability*, p.909, Dodman, D. et al. 2022). The diagram below from the IPCC shows how high the potential of implementation of solar and wind energy are likely to mitigate climate change, notably, solar has the highest potential as well as the highest measure of uncertainty due to its variance.

Notably, the figure also lists the most relevant factors for reducing net emissions in the building sector, which are dedicated to the materials used in construction and the possibility of renewable energy production. Although new buildings with higher energy standards is the highest individual contribution

option in contributing to decarbonization, in the context of comparable alternatives it has the highest cost in terms of carbon emissions. Retrofitting existing buildings to reduce energy demand and utilize efficient building systems offer significant contributions at low carbon cost. In order to make any impact on net emission reduction from the planning discipline, it is vital to understand the intersection between the building and energy sectors.

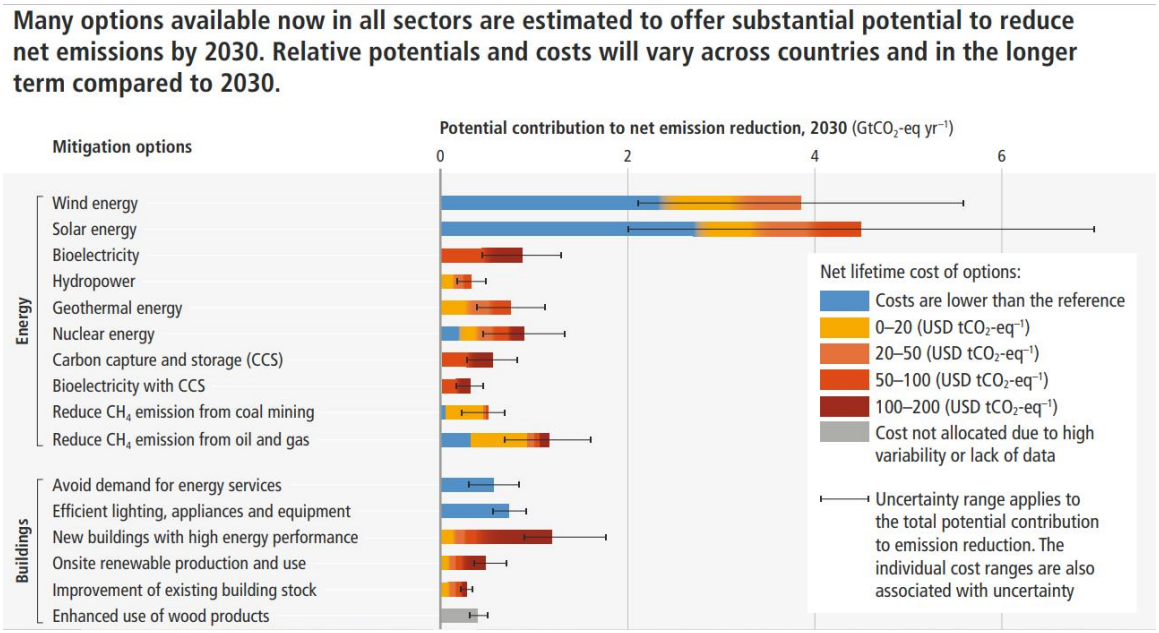

Figure 13: IPCC 2022 Factors Reducing Net Emissions in Building and Energy Sectors

On the large scale, solar applications involve numerous stakeholders who interact with one another in various ways. For more complicated systems, such as building integrated photovoltaics (BIPV), the interactions between stakeholders become even more complicated. The figure below shows the interactions between stages of a development, challenges at each stage and relevant stakeholders. Many renewable systems face similar ranges of challenges necessitating cooperation between different stakeholders to progress.

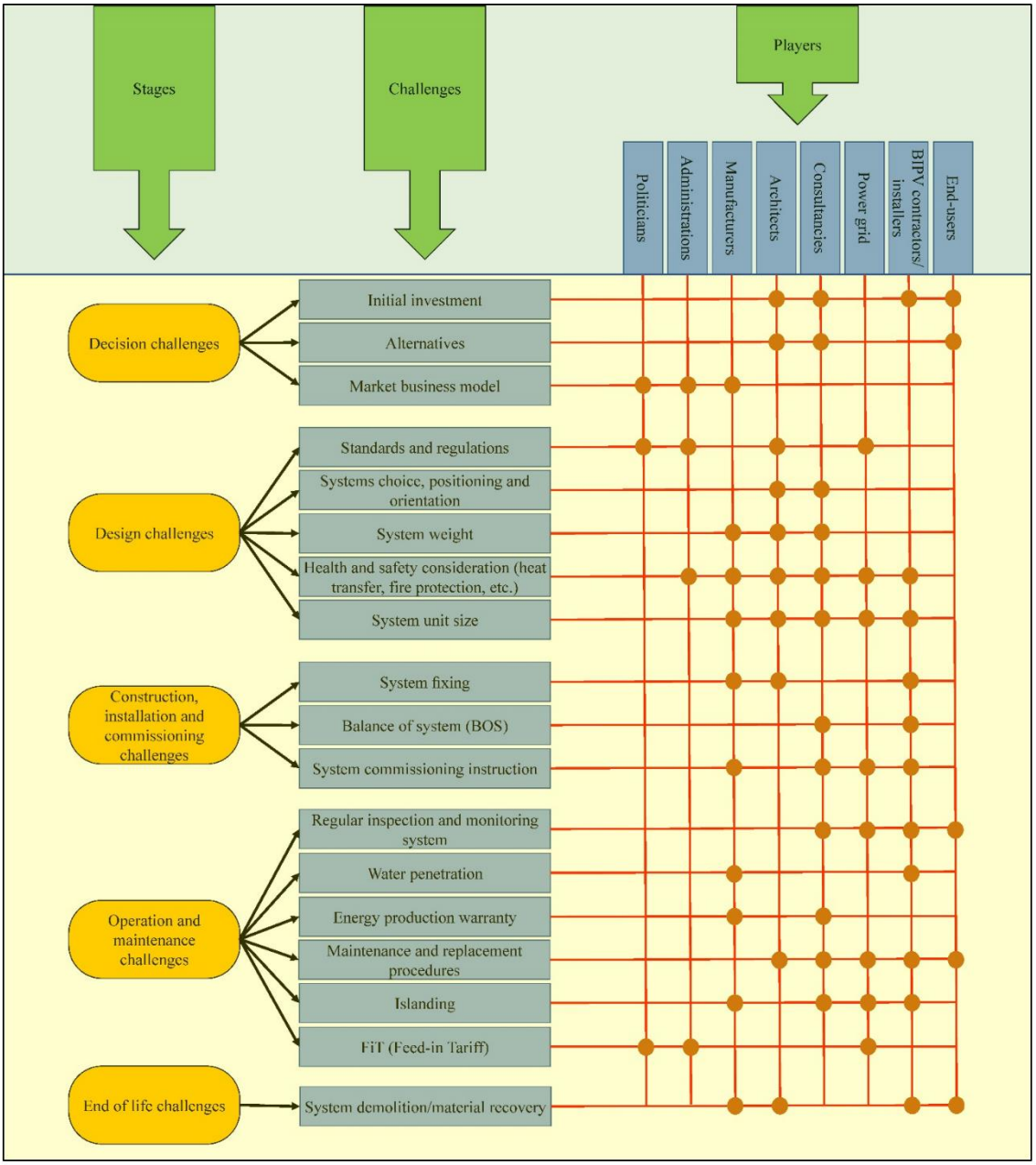

Figure 14: BIPV barrier classification and involved stakeholders who can contribute to the solutions.

Regardless of the purpose and ownership of the buildings, part of maintaining aging buildings while they inevitably age is adhering to the most recent building codes for the area. As buildings consume large amounts of electricity in regular intervals, increasingly strict building regulations are

developed to avoid preventable waste by making buildings more sustainable overall.

To this end, the Energy Performance of Buildings Directive for the European Union includes many specific guidelines for new building construction and renovation of existing buildings. Participating countries must “establish long-term renovation strategies, aiming at decarbonising the national building stocks by 2050” and “set cost-optimal minimum energy performance requirements for new buildings, for existing buildings undergoing major renovation, and for the replacement or retrofit of building elements like heating and cooling systems, roofs and walls.” (Energy Performance of Buildings Directive, n.d.). More directly, most recent revision from December of 2021 mandates that “all new buildings must be nearly zero-energy buildings (NZEB) and since 2019, all new public buildings should be NZEB” which must have established solutions and pass inspections for each such structure sold, rented, or preparing for significant renovations (Energy Performance of Buildings Directive, n.d.). Furthermore, provisions mandate that member countries “must make energy efficient renovations to at least 3% of the total floor area of buildings owned and occupied by central governments” to promote energy efficient buildings over comparable alternatives (Energy Performance of Buildings Directive, n.d.). Many other countries have committed to similar goals, though pursued in slightly different ways. Although not a universally applicable or complete solution on its own, solar energy can contribute to meeting this goal in combination with other mitigation strategies.

Common Policy Incentives

There are many policies that determine how energy individually generated by solar systems is distributed to the surrounding electrical grid are described as follows. Feed-in tariffs (FiTs) provide a fixed payment or premium rate to solar energy producers for the electricity they generate and feed into the grid. In these systems, all electricity generated is directly sold to the electrical grid and the producer must still pay for the utility separately. Comparatively, net metering allows solar energy system owners to feed excess electricity they generate into the grid in exchange for credits or financial compensation for the surplus energy. This promotes self-consumption and provides an incentive for individuals and businesses to install solar systems. Power purchase agreements (PPAs) involve long-term contracts between solar energy producers and utilities, where the utility agrees to purchase the electricity generated by the solar system at a predetermined price. These agreements provide revenue certainty for solar project developers and encourage the deployment of utility-scale solar projects. A final, a less targeted approach is the option for government entities to offer tax incentives, subsidies, and grants, to incentivize individuals or businesses to independently invest in solar energy systems.

Chapter 3: Lines of Latitude

The consistency of solar radiation across the globe is consistent with lines of latitude, measuring how far north and south a location is from the equator. Although the Earth's tilt on its access varies slightly in its revolution around the sun throughout different points of the year, the degree of incidence, or the angle at which sunlight strikes a surface can be calculated quite accurately using the latitude of a given location.

In reference to sun angles during short, winter days are low in the sky compared to the higher angle during the longer summer days. The dates that are used later in the paper are the summer solstice for the solar maximum, the winter solstice for the solar minimum, and the equinoxes for the solar average. As the sun angle is the same on both dates, any location in full sunlight on these two dates is, at a minimum, be in full sunlight for the half of the year between vernal and autumnal equinoxes. The figure below shows, the variation in sun angle at those three key points throughout the year.

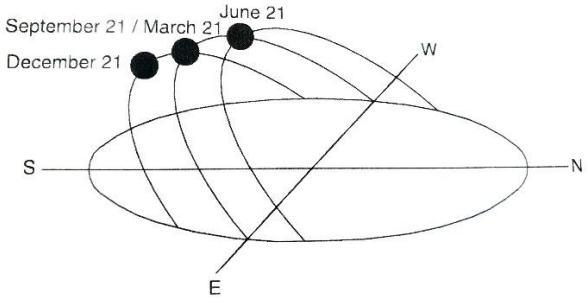

Figure 15: Annual changes in the sun's position in the sky (northern hemisphere)

On the cosmic scale, the Earth's axial tilt varies slightly over very long periods of time. For the purposes of the scale of this study, a consistent measured value is approximately 23.45° and is used as a constant throughout. This factor of planetary movement creates three primary climate zones of tropic,

temperate, and polar zones. Locations within 23.45° of the equator receive the most direct sunlight consistently throughout the year, creating the tropic zone between the boundaries of the Tropic of Cancer north of the equator and the Tropic of Capricorn south of the equator. Measured from the north and south pole to approximately 66.5° of the equator, forms the Arctic circle in the north and the Antarctic circle in the south. The resulting temperate zones are in between the polar and tropic zones.

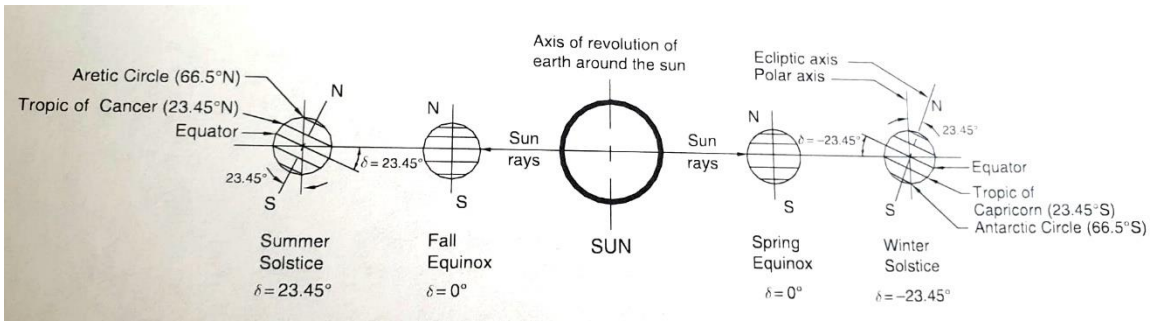

Figure 16: Yearly variation of solar declination angle

Two other relevant variables are shown in the following diagram. These are the solar altitude “angle between the line joining the center of the solar disk to the point of observation at any given instant and the horizontal plane through that point of observation” and the solar azimuth “angle between the north-south line at a given location and the projection of the sun-earth line in the horizontal plane” denoted as α (alpha) and z, respectively, in the following diagram (Elsevier, 2012). It should be noted that the value for the solar azimuth is always 0 at solar noon, as this is the point when the sun is oriented due south. In later chapters, azimuth is used to refer to the angle of rotated street grids to calculate solar potential of surfaces not directed due south. The azimuth is applied to shading angles at different points throughout the year due to the changing angle of the sun. All calculations are presumed to be measured at solar noon so that the solar azimuth is 0 regardless of the azimuth of the building or street rotation.

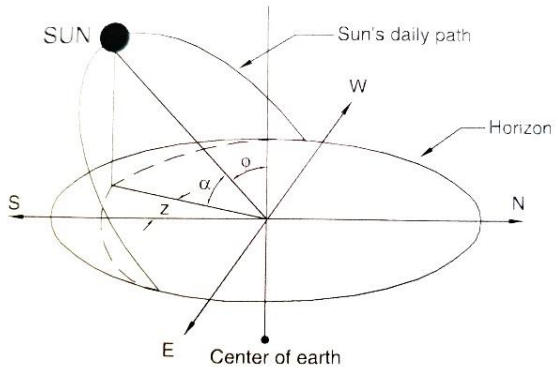

Figure 17: Apparent daily path of the sun across the sky from sunrise to sunset

These factors of sun position create the seasonal variation of hours of sunlight as well as the amount of irradiation directed to a location, which contributes to the calculations that are used in later sections. A location's latitude also determines the sun's angle at various points throughout the year, with higher variability further from the equator.

Figure 17 shows, in elevation, a simple configuration of buildings on the at solar noon on the equinox in six different locations in the northern hemisphere with lines of shading dependant on latitude. The ratio of building height to street width used in the following diagram is explored in greater detail in later chapters. Here, it is only relevant to state that two buildings orthogonally oriented with Building A facing south and Building B projecting shade onto its surface. Each line represents the lowest line of direct beam radiation striking the surface of the south facing building due to shading from the adjacent building. Areas below each line are therefore shaded, dependant on diffuse or reflected radiation from that point down.

The vertical surface of building A would be in near constant shade if it were found in Oslo, compared to the near constant, direct sunlight if it were found in Singapore. Likewise, the top three floors would receive direct sunlight in Hong Kong, but only the top floor would receive direct sunlight if it were in Tokyo instead. This serves to illustrate how the planning strategies of an area must take into account the latitude of a location to efficiently plan for solar installations best suited for beam radiation.

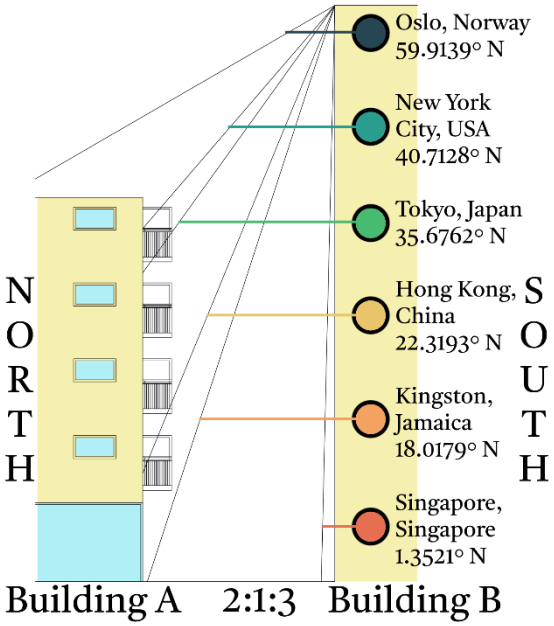

Figure 18: Equinox angles by latitude

Solar radiation can be divided into three main categories of “beam radiation” otherwise known as “direct beam radiation”, “diffuse radiation”, and “reflective radiation”. The first describes solar radiation in a straight line traveling from the sun to the Earth’s surface. Most of the solar radiation on sunny days with little to no cloud cover is direct radiation. Days with thick cloud coverage lower the beam radiation to zero. Diffuse radiation, sometimes called sky radiation, is caused by atmospheric conditions that scatters particles and molecules throughout all regions of the sky along their path to the surface of the Earth. As a result, “the amount of diffuse radiation is up to 100% of the total radiation for cloudy skies and 10% to 20% of the total radiation for clear skies.” (Gholami et al., 2021). Reflected radiation is caused by the reflection of direct and diffuse radiation on other surfaces, although the overall contribution is quite minimal. However, if the collector is tilted at a steep angle from the horizontal,

as is the case with vertical building façade installations, the reflected radiation is higher. A study of BIPV materials found that “that in climates with higher diffuse radiation, the contribution of IR radiation decreases” suggesting that “organic and dye-sensitised solar cells could be a good option for a cloudy climate since they have a more stable performance even in such a climate.” (Gholami et al., 2021). As climate and temperature is a significant influence on the various components of solar irradiation, the solar technology most suited for that environment must be applied to maximize the potential energy from incident solar radiation. As a result, shading diagrams showing the angle and path of the sunlight signify the line of direct radiation, as reflective radiation and diffuse radiation are generally more diminished.

Chapter 4: Street Orientation

A city's streets, paths, and transit lines form the special networks that shape a complex urban system. "Measuring these network patterns can help researchers, planners, and community members understand local histories of urban design, transportation planning, and morphology; evaluate existing transportation system patterns and configurations; and explore new infrastructure proposals and alternatives. It also furthers the science of cities by providing a better understanding of urban patterns and how they correspond to evolutionary mechanisms, planning, and design" (Boeing, 2020). Historically, geography has presented many challenges to consistently measuring and evaluating such large and varied areas; although this difficulty has been combatted substantially with digital mapping tools. An aid to visualizing the proportional relationship between streets and the built environment is exemplified in figure-ground maps. In these, the white represents transit corridors, compared to the black representing the areas those streets serve. The following diagram is part of an examination of street networks within a square mile of some of the largest and most populous cities.

All cities adjust to their geographical constraints, such as those of surrounding waterways and changes in elevation. Depending on the climate of a given area, these factors can contribute to urban heat island effects through air circulation and passive solar heat gain. As the problem of urban sprawl has become a more prevalent issue with the thoughtful management of land resources, more modern established cities tend to grow in more regular, measured developments.

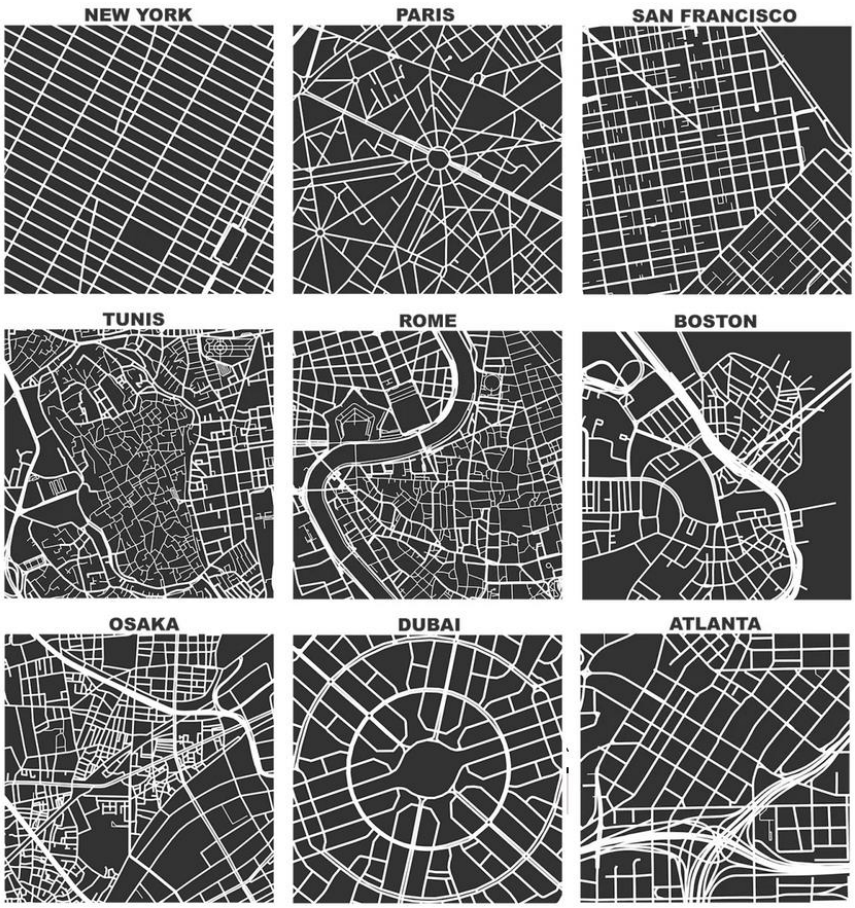

Figure 19: Square-Mile Street Network Visualization

Older cities that have largely grown organically often struggle to adapt to population expansion and the necessary supporting infrastructure. Cities seeking to preserve specific historically significant structures do so at the cost of wrapping somewhat irregular connection systems around them at the cost of better mobility efficiency. Changes in mobility systems over time likewise impact street layouts, as those originally designed for navigation by pedestrians struggle to widen streets to accommodate vehicles and similar larger scale transit systems. While this does not completely prevent alterations, it does serve as a detriment to make the process more arduous and often limit the scope of potential development. More regular streets make it easier to predict consistent shading patterns, while curving streets create a wider range of variability. For the purposes of large scale solar installations in these urban

centers, the increased variability of curving streets presents added complications in processing a consistent solar potential, both in surrounding shading structures and the variability of irradiation due to the solar azimuth.

This study *Urban spatial order: street network orientation, configuration, and entropy* measured street lengths and direction to create a matrix of relevant factors. Of these, the variable φ denoted a value between 0 and 1 which indicates a normalized measure of orientation-order where lower values denote low order to perfectly ordered, uniform grids. One finding from this examination was that “cities with higher φ values also tend to have higher node degrees, more four-way intersections, fewer dead-ends, and less-winding street patterns. That is, cities that are more consistently organized according to a grid tend to exhibit greater connectedness and less circuity” (Boeing, 2019). Relating to the application of urban solar installations, this examination of street geometry is useful for determining a scale for solar calculations, as simplifying the street direction also denotes the directionality of the city blocks hosting those installations. For cities with a higher degree of order, the factor of solar azimuth can be applied with consistency across large areas, while those with a lower degree of order must be completed within an individual area of street grid rotation.

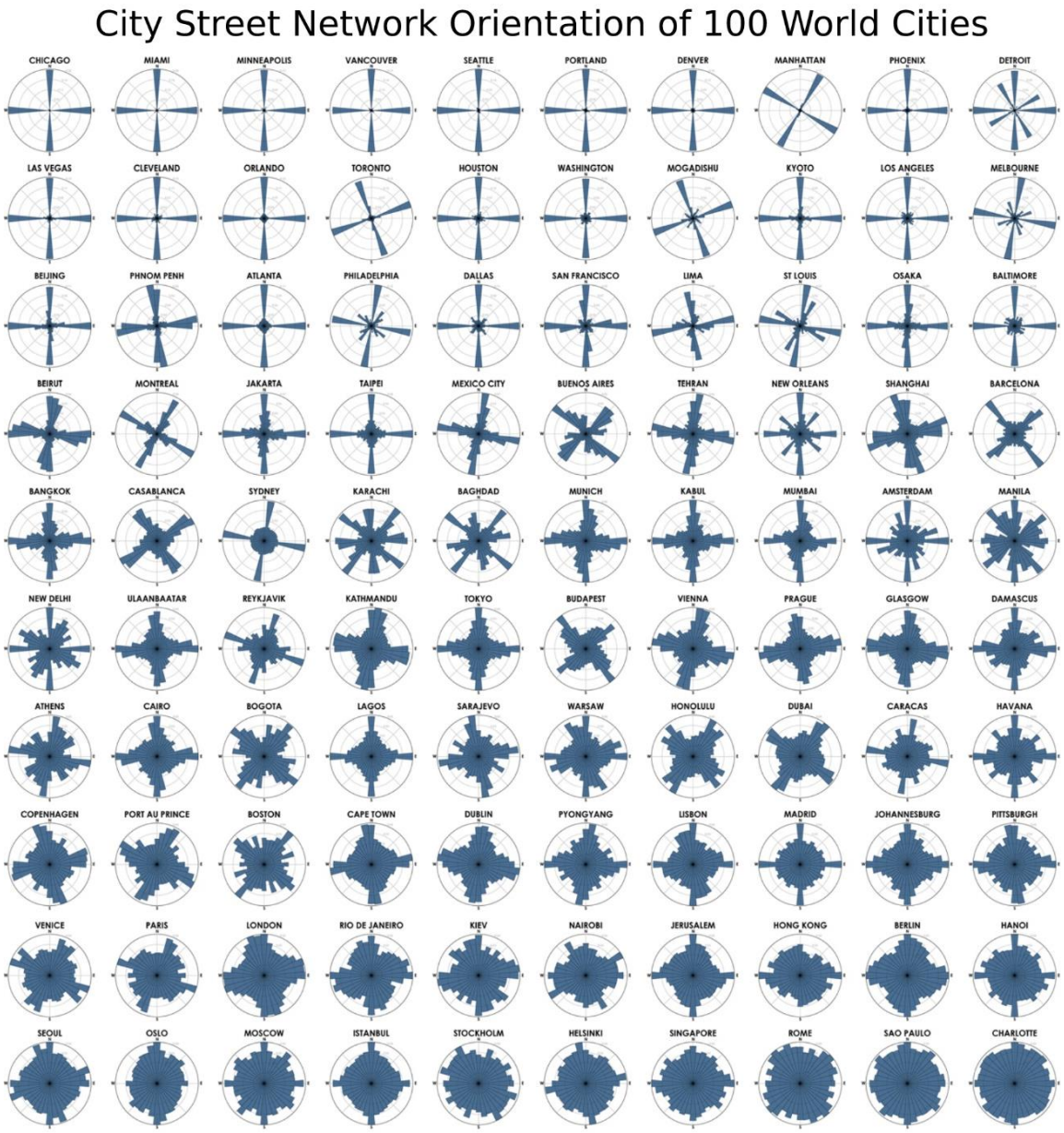

Figure 20: City Street Network Orientation of 100 World Cities

Case Study: Comparison of Barcelona and New York

Given that the two locations are close in latitude, how does the difference in street rotation between effect the shading of surrounding vertical surfaces? Which of the two block arrangements, square or rectangular, is more suitable for vertical solar installations based on lowest levels of surface shading?

Summary Answer: Even small variations in latitude can produce a difference of solar potential. There is a 0.68° difference in latitude and 18° difference in street rotation. Approximately equilateral street rotation produces lower levels of direct sunlight or direct beam radiation. More disparate angles produce higher direct beam radiation on surrounding surfaces. The difference is slight for square configurations, with a variance of 1.5%, and greater for rectangular configurations, with a variance of 23.9%.

The following two cities, from a design standpoint, have an interesting array of similarities and differences that merit examination by comparison. The first is that, despite the distance between their locations, they are very close in latitude. Barcelona is located at the latitude of 41.39° N, while New York City is located at the latitude of 40.71° N, a difference of 0.68 degrees between the two. To show greater variance, solar elevation angle for these locations the winter solstice is used. This is the lowest solar angle of the year which, likewise, produces the longest shadows, producing greater variance for comparison. As described in Table 1, this angle is calculated as follows where 23.5 represents Earth's Axial Tilt.

$$\textit{Solar Altitude Angle at Winter Solstice} = 90 - (\textit{Degree of Latitude}) - 23.5$$

Building azimuths in this case study are measured with integers ranging from the value of 0 for facades directed due south, -90 for east facing values, and 90 for west facing values.

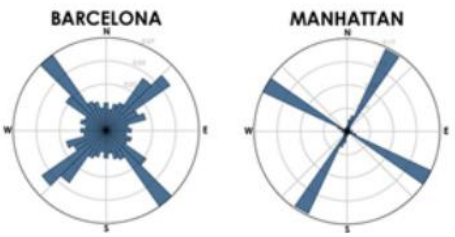

Portion of previous figure

The street grid of Barcelona is rotated from an orthogonal, north to south axis with the southwest façade measured around 44° and the southeast façade measured around -46°. In contrast, the selected area of the New York City street grid, specifically part of Manhattan, is rotated with the southwest façade measured around 62° and the southeast façade measured around -28°. The adjacent diagram to the right isolates these same two cities from the previous Figure 20 for side-by-side comparison, showing both the rotation of streets and degree of order. The following diagram showcases the rotation of the two areas at the same scale at a given point of examination.

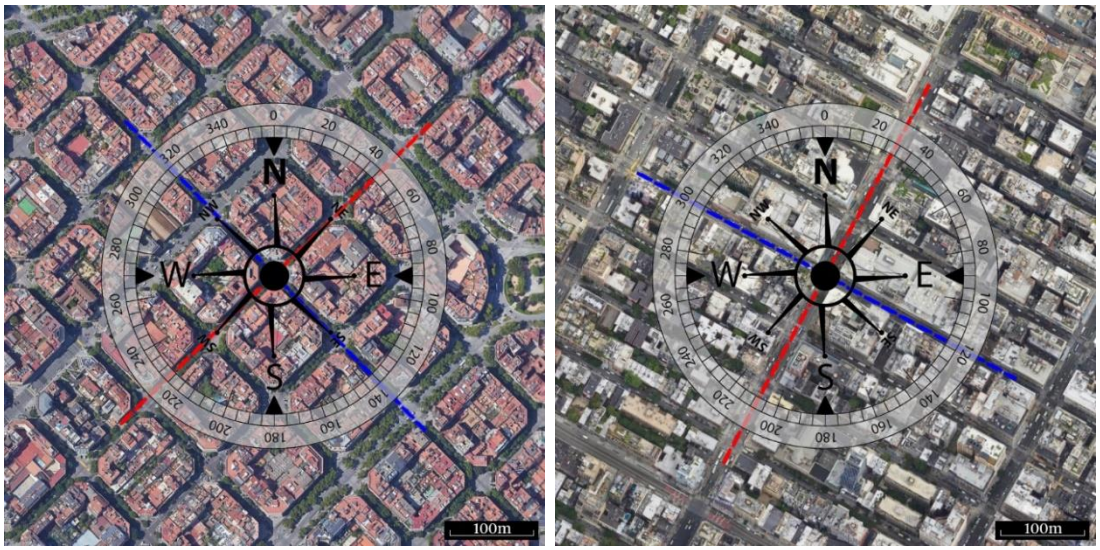

Figure 21: Street rotation of two cities

As the following calculations focus on the impact of street rotation, the given value of 16 meters of height is used for both areas to compare similar city blocks by simplifying the variables. Distance between these blocks including a

combination of streets, sidewalks, and other spacing features is denoted as an overall measurement of street width. Approximate values of 20 meters for Barcelona and 16 meters for New York City are used for these respective distances based on observations of these areas in GIS (Geographical Information System) for mode values rounded to a whole number integer. These variables are shown in Table 2 below.

Table 2: Barcelona and New York Comparison 1

		Degrees From Equator	Solar Elevation Angle at Winter Solstice	Building Azimuth SW	Building Azimuth SE	Height	Street Width
Origonal Orientation	Barcelona, Spain	41.39	25.11	44	-46	16	20
	New York City, USA	40.71	25.79	62	-28	16	16

Applying the method of calculating shadows shown in Figure 4 in the methodology section with these given variables can be used to show the difference in shading of the surrounding surfaces. At the points used in this study, Barcelona's blocks are nearly square with southwest and southeast façades being nearly equal, while New York blocks on the southwest façades are over four times longer than the corresponding southeast façades. The Barcelona building azimuths is such that each side is a near equal rotation from the orthogonal layout, casting shadows of near equal length on surrounding surfaces. The New York City building azimuths are more dramatic difference with the smaller face rotated an acute angle from due south and the longer face rotated a complementary obtuse angle. From here, Table 3 compares both configurations in their original state, then both rotated to the same amount as the New York area and the rotation of the Barcelona area for comparison to find

which configuration allows more direct sunlight and, correspondingly, more direct beam radiation on surrounding surfaces.

Table 3: Barcelona and New York Comparison 2

	Original Orientation		Both Blocks New York Orientation		Both Blocks Barcelona Orientation	
	Barcelona, Spain	New York City, USA	Barcelona, Spain	New York City, USA	Barcelona, Spain	New York City, USA
Degrees From Equator	41.39	40.71	41.39	40.71	41.39	40.71
Solar Elevation Angle at Winter Solstice	25.11	25.79	25.11	25.79	25.11	25.79
Building Azimuth Southwest	44	62	62	62	44	44
Building Azimuth Southeast	-46	-28	-28	-28	-46	-46
Height	16	16	16	16	16	16
Street Width	20	16	20	16	20	16
SW Height in Direct Sunlight at Winter Solstice (m)	13.03	16.00	16.00	16.00	13.03	10.75
SE Height in Direct Sunlight at Winter Solstice (m)	13.49	8.76	10.62	8.76	13.49	11.13
SW Edge (m)	115	244	115	244	115	244
SE Edge (m)	100	56	100	56	100	56
Facade Area In Direct Sunlight (m^2)	2,848	4,394	2,902	4,394	2,848	3,245
Total Facade Area	3,440	4,800	3,440	4,800	3,440	4,800
Percentage in Sunlight	82.8%	91.5%	84.3%	91.5%	82.8%	67.6%

Building height in direct sunlight (measured from top of building) =

((Street Width / Cos(Rotation Angle)) Tan(Solar Azimuth Angle))*

Height in direct sunlight = ((Ws / Cos(z)) Tan(α))*

These findings show that street orientations rotated approximately equilaterally, such as that of the Barcelona street grid, have the lower levels of direct sunlight or direct beam radiation, regardless of whether the buildings are arranged in square or rectangular configuration. Those same configurations with more disparate angles, in this case, that of the New York City street grid, produce higher surrounding sunlight and direct beam radiation on surrounding surfaces. The difference is slight for square configurations, with a variance of 1.5%, and greater for rectangular configurations, with a variance of 23.9%. These proportional relationships could contribute to either increasing the exposure of vertical solar installations to direct beam radiation or reducing passive heating by maximizing shading to vertical surfaces. The impact of the relationship between building height and intermittent spacing will be explored in greater detail in Chapters 7 and 8.

Chapter 5: Solar Glazing

What is Solar Glazing?

The overall idea of transparent solar panels is relatively new and difficult to achieve in practice. Many variants of this technology have been developed, but each encounters the issue that the more transparent the surface, the lower the efficiency of converting light to electricity. The company Ubiquitous Energy has developed what they claim to be a the first truly transparent, unstinted coating applied to windows to make a transparent solar panel. As shown in figure 21, this process, called "UE Power^{TM}", in transparent solar panels allows more visible light to pass through while converting a range from the ultraviolet to infrared portions of the light spectrum into useable electricity. Although their specific efficiency is not stated, it is estimated that transparent solar panels operate at around half the efficiency of standard panels. As previously mentioned, the efficiency used is 7% for all relevant case studies, as this is a value observed with some consistency in solar glazing models. Obviously, similar models with improved efficiency yield significantly higher energy.

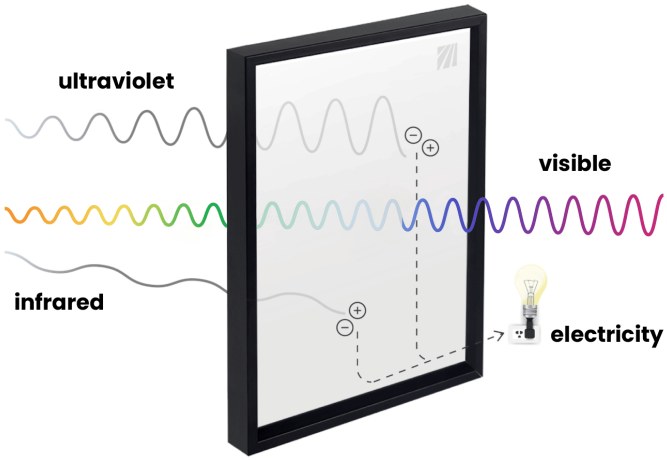

Figure 22: UE PowerTM

As of the writing of this thesis, this specific product is only available to be applied to new or replacement window products, although the company hopes to achieve the ability to apply this to existing windows in the future (Ubiquitous Energy, 2023). The case study at the end of this chapter assumes that the

technology applied to the existing windows or as part of a larger replacement in a theoretical retrofit.

Skysrapers as Inefficient Buildings

The idea of modern skyscrapers often evokes the image of curtain walls of glass and steel on all sides, sometimes called “international style” for the architectural ideals of the design. Structural supports are placed closer to the building’s center, hidden behind the presentation of a façade that appears much lighter than a building of that scale would require. Although this brings extensive natural lighting into the building, conventionally, this also allows a substantial transference of thermal energy through the windows. Consideration for materials can mitigate the effects of passive solar heating’s impact on a building’s internal environment, such as applying higher rated insulation and windows that are double or triple paned, especially on the sides of the building with the most solar irradiance. Even so, unshaded windows are a lower insulation value than standard walls, allowing significantly more thermal transferral. A common solution for this issue has been a combination of powerful air conditioning, ventilation, and heating systems, all of which require a high amount of the building’s total energy usage to operate. In the lifetime of the building, the consequences this design decision is passed on to the building’s occupants in the form of increasing operational expenses as the supporting systems age and, more recently, as tariffs in areas with building or zoning regulations targeting buildings with inefficient energy use and excessive carbon emissions.

In *Green Retrofitting Skyscrapers: A Review*, author Kheir Al-Kodmany lists the many common methods of retrofitting skyscrapers in addition to the possibility of on-site energy generation. While not be explored in detail, it is worth noting that this list includes changes to building systems including lighting, water, heating, ventilation, air conditioning, building automation systems, and overall increased insulation applied in various combinations to lower the overall energy demand. Also inherit to the design of skyscrapers is that, although they cast large shadows, surfaces located closer to the top of the structure receive far less shading from surrounding structures, compared to their bases, which are more frequently shaded. This provides many opportunities for roof and large scale vertical solar applications. In the cases of international style skyscrapers with façades of high to near continuous window coverage, there are limited mounting surfaces for conventional solar installations compared to the consistency possible in a solar window alternative. As buildings must change to meet new energy standards, the most wasteful buildings must undergo the most renovations.

Research Question: How much energy would be generating by replacing half (all southwest and southeast facing windows) in the Empire State Building with solar glazing? How much energy would be generated by replacing the entire glazed façade on the southwest and southeast of the Seagram building with solar glazing? Could this be viable for transforming skyscrapers into zero energy or energy plus structures?

Summary Answer: The Empire State Building scenario found that solar glazing could supply approximately 1.27% of the estimated energy consumption of the building.

The Seagram Building scenario found that solar glazing could supply 2.63% of the estimated energy consumption of the building.

These case studies show that, due to the low efficiency of solar glazing systems, they contribute to the building's energy demands, though not significantly enough to transform the buildings into nearly zero energy buildings alone.

As displayed the previous chapter on street orientation, for these calculations the solar azimuth is measured from where 0 is facing due south. Both buildings are located in an area of the Manhattan street grid rotated in the same way as shown in figure 18 so that the southeast azimuth is about -28° and the southwest azimuth is about 62°. As the windows are vertical, they are mounted at 90° from the horizontal. Inputting both of these factors into the online database tool for the European Union's Photovoltaic Geographical Information System along with the location yields the approximate values of 1099 kWh/m^2 for the southeast side and 897 kWh/m^2 for the southwest side. Where specific values were unavailable, estimations based on publicly available sections, floor plans, and photographs, were applied to extrapolate approximate values used in these calculations.

Case Study: Empire State Building

The Empire State Building was selected for this case study both for its international renown and for its active role in pioneering large scale retrofits to encourage the green energy transition. The Empire State Building was first opened in 1931. However, due to the aging building systems and low energy standards of the time of its construction, a group of public and private stakeholders undertook the challenge of increasing the building's efficiency in preparation for stricter energy regulations, such as those discussed in chapter 2. The unprecedented scale of transformation was used as a demonstration of feasibility and a call to action for environmentally conscious urban design and retrofits for the long-term survival of the planet (De La Garza, 2021). The Empire State Building and similar structures "represents a huge obstacle to cities' dreams of carbon neutrality. New York City's buildings account for 70% of its carbon emissions, for example, and half of those emissions are produced by the largest 5% of its structures." (De La Garza, 2021).

The extensive retrofit was completed in 2010, included refurbishing each of the 6,510 windows from their original single pane into an effectively triple-glazed pane to reduce heat loss (Al-Kodmany, 2014). "All told, the upgrades have cut the building's energy usage by about 40%, saved its owners more than $4 million every year and played a part in attracting high-value tenants that have fattened the building's bottom line." (Al-Kodmany, 2014). "This portion of the upgrade, however, only represents about 13 percent of the project's reduction." (Climatewire, 2010).

This is relevant to show that a theoretical large scale renovation to apply a solar coating to windows is similar to an action completed in the most recent

retrofit while also furthering the stated goals that led to that very retrofit. It is not beyond the realm of possibility to suppose that the same group of stakeholders may view this as favourable should solar glazing systems pass the tipping point of a cost-benefit analysis to become the focus of a future retrofit.

Due to the building's orientation, half of the total 6,510 windows face either southwest and southeast. Of these 3,257 windows, from building proportions estimates and windows counted over a sixty story area between the and floors, for each window on the shorter, southeast face, there are 1.4 windows on the longer, southwest face. By this proportion, it is estimated that 1,348 are located on the southeast side and 1,909 on the southwest side. From an estimation of the approximate size of a consistent pattern of windows, the dimensions of four feet by five feet, or twenty square feet (about 1.86sqm) is applied per window. It should be noted that the following calculations do not take into account shading or that areas such as the observation deck have windows of a different size.

$$(SE\ or\ SW\ window\ count\ \times window\ area(m^2)) \times$$

$$SE\ or\ SW\ irradiation\ (kWh/m^2) =\ SE\ or\ SW\ Solar\ Irradience\ kWh$$

$$(Total\ SE\ kWh +\ Total\ SW\ kWh) \times\ 7\%\ Efficency$$

$$=\ Energy\ Generation\ (kWh)$$

$$\frac{Total\ kWh}{1000} = Total\ Mwh$$

The Empire State Building has a floor area of 2,248,355 sqft (208,879 m^2) (*Empire State Building - the Skyscraper Center*, n.d.) and the estimated average energy consumption by commercial buildings in the United States measured in 2012 by floor area is 15.9 kwh/sqft (171.15 kwh/sqm) (*EIA*, 2016).

Combining these two figures yields an estimation that the Empire State Building consumes around 32,700 Mwh by floor area, not accounting for the inefficiency of the original system or the improvements of the recent retrofit. By these estimations, the result is that 6,052m^2 yields 415.51MWh of electricity, or an estimated 1.16% of the building's estimated energy usage.

Table 4: Empire State Building Calculations

Empire State Building		
Window Area (m^2)	1.86	
	South East	South West
Window count	1,348	1,909
Total Area (m^2)	2,505	3,547
Solar Azimuth	-28	62
Irradiation kWh/m^2	1,099.01	897.42
Solar Irradiance (kWh)	2,752,652	3,183,182
Account for 7% efficency (kWh)	192,686	222,823
kwh/1000 = MWh	192.69	222.82
Total Solar Glazing Energy	415.51	Mwh
Building size	208,879	m^2
Average energy use per sqm	171	kwh/m^2
Total energy use	35,749,641	kwh
Building Total Energy Use	35,750	Mwh
Percent Energy from Solar Glazing	1.16%	

Case Study: The Seagram Building

The Seagram Building is considered one of the earliest skyscrapers pioneering the modern style for which this and other buildings by architect Mies van der Rohe became well known for. It was constructed between 1954-1958, is "157 meters high, spread over 39 floors" primarily dedicated to offices (*Seagram Building - Data, Photos & Plans - WikiArquitectura*, 2020). Due to the tall, inset first floor, 8m is disregarded from the building's height. From the

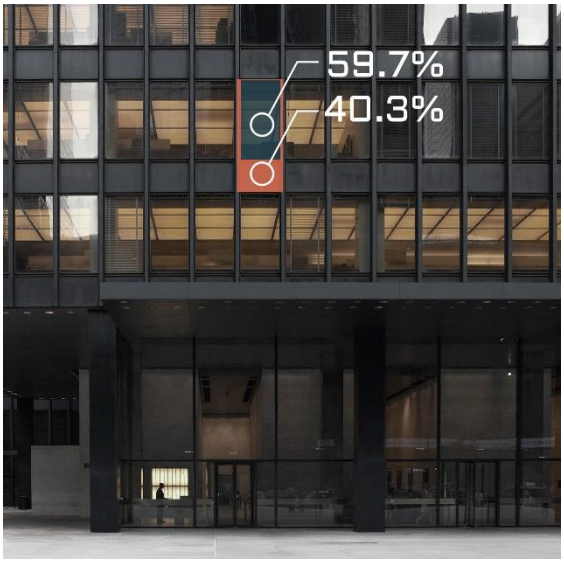

Figure 23: Seagram Building Windows

building information in QGIS, the footprint of the building is 200ft (60.96m) along the southwest façade by 290ft (88.392m) along the southeast façade. Rather than counting windows, this case study will use a simplified façade analysis to estimate the total window area. The building's façade is a repeating pattern of windows within metal frames. The diagram to the right shows the proportional relationship between each window and the frame it is set within. In this case, in the repeating pattern of glazing, 59.7% is window area to the 40.3% area of the frame.

The resulting calculations are as follows. Transforming 13,285m^2 into solar glazing will result in a projected 945.51Mwh of electricity. Disregarding shading, insulation, and the building's maintenance systems, the estimated energy use of this building is 35,967Mwh based on floor area. Transitioning these two facades of the building into solar glazing could contribute to 2.63% of the building's overall energy demand.

Table 5: Seagram Building Calculations

Seagram Building		
	South East	South West
Facade Length (m)	88.4	61.0
Facade height, ex. first floor (m)	149	
Vertical area (m^2)	13,170	9,083
Percent facade windows	59.7 %	59.7 %
Adjusted area	7863	5422
Solar Azimuth	-28	62
Irradiation kWh/m^2	1099	897
Solar Irradiance (kWh)	8,641,016	4,866,211
Account for 7% efficency (kWh)	604,871	340,635
kwh/1000 = MWh	604.87	340.63
Total Solar Glazing Energy	945.51	Mwh
Building size	210147	m^2
Average energy use per sqm	171	kwh/m^2
Total energy use	35,966,604	kwh
Building Total Energy Use	35,967	Mwh
Percent Energy from Solar Glazing	2.63%	

Chapter 6: Rooftop Solar

As discussed in chapter 1, rooftop solar is a flexible technology that can be applied to a variety of locations while also minimizing impact from mitigating factors, such as shading and aesthetic appeal due to their placement. For this reason, industrial and retail areas that typically operate in low-density areas occupying a substantial footprint area are well suited for rooftop solar, especially when the roofs are flat or simple, sloped roofs. For the purposes of this thesis, low-rise structures are defined here as three or fewer stories. Furthermore, given the generally low height of industrial areas, there is little advantage to vertical solar installations while simultaneously well suited for rooftop solar. These arrays can be seamlessly incorporated into existing roof structures in the form of flat roofs, pitched roofs, or even as shading devices in the form of solar canopies due to the flexibility of the technology. In the case of flat roofs, installations can be directed to the optimal direction and azimuth.

From an aesthetic standpoint, there is far less resistance to the adoption of rooftop solar than other integrated renewable technologies as it is so completely removed from the observation and experience of the general public. From a planning standpoint, converting the roofs of industrial areas serves to densify an area by combining a developed area with the function of energy generation comparable to solar farms occupying a similar area.

Research Question: Can solar roofs transform two Ikea locations in the Oslo area into net zero energy buildings or energy positive buildings?

Summary Answer: Within a range of 15%-20% efficiency solar panels covering 80% of the roof area in solar panels yields 23% to 31% of the building's estimated energy needs based on building area in both locations.

Ikea Furuset would need between 21,835 sqm and 32,342 sqm, while Ikea Slependen would need 30,272 sqm to 44,838 sqm of additional solar arrays to become net zero energy buildings. From the cite's gross area, this is achievable for Ikea Furuset, but not Ikea Slependen to reach with carport solar roofs or similar systems.

Ikea retail locations follow a consistent design structure a two-story warehouse style structure with a flat roof occupying a large footprint surrounded by an extensive parking area. These low-rise structures (here defined as of or below three stories or 16 meters) have limited vertical area for vertical solar installations, but abundant rooftop area.

As a company policy, Ikea has stated a commitment to sustainable building and operation practices. Aside from investing in various renewable energy systems, the company has also set specific goals for all retail locations to be "powered by 100% renewable energy while increasing energy efficiency by 2025" (IKEA Newsroom, n.d.). The Country Sustainability Manager for IKEA Retail in the U.S. stated in the same article that "54 rooftop solar arrays atop 90% of [the] IKEA U.S. locations" are currently in operation (IKEA Newsroom, n.d.). In addition to rooftop solar, the recent additions of solar car park coverings

in Maryland has proved substantial energy returns “equating to a 57% energy cost savings for the store.” (IKEA Newsroom, n.d.).

Table 6: Ikea Calculations 1

Ikea Furuset			
Gross Lot Area	43,505	Number of Floors	2
Building Footprint (m2)	12,107	Building Area (m2)	24,214
Floor Area Ratio (Density)	0.56	Estimated Building Demand (Mwh)	7,264
Average EU Energy (kwh/m2)	300		
Percent of Roof Used	80%	Roof Solar Area (m2)	9,686
Solar Potential (kwh/m2)			1,152
Efficency	15%	Efficency	20%
Total Roof Radiation (MWh)	1,674	Total Roof Radiation (MWh)	2,232
Building Solar Supply	23%	Building Solar Supply	31%
Unoccupied Lot Area (m2)		31,398	m2
Additional Solar Area to Reach Net 0 (m2)			
15% Efficency	32,342	20% Efficency	21,835

Table 7: Ikea Calculations 2

Ikea Slependen			
Gross Lot Area	25,725	Number of Floors	2
Building Footprint (m2)	16,785	Building Area (m2)	33,570
Floor Area Ratio (Density)	1.30	Estimated Building Demand (Mwh/m2)	10,071
Average EU Energy (kwh/m2)	300		
Percent of Roof Used	80%	Roof Solar Area (m2)	13,428
Solar Potential (kwh/m2)		1,152	
Efficency	15%	Efficency	20%
Total Roof Solar (MWh)	2,321	Total Roof Solar (MWh)	3,095
Building Solar Supply	23%	Building Solar Supply	31%
Unoccupied Lot Area (m2)		8,940	m2
Additional Solar Area to Reach Net 0 (m2)			
15% Efficency	44,838	20% Efficency	30,272

These calculations use the European Union annual specific energy consumption 300 kWh/m^2 for commercial buildings to estimate the building’s

energy use by area (*Progress on Energy Efficiency in Europe*, n.d.). The irradiation value from the PVGIS database of 1152.29kwh/m^2 measured in Oslo and with optimized direction and azimuth (JRC Photovoltaic Geographical Information System (PVGIS) - European Commission, 2016). The building boundary area was exported from QGIS to Autocad to calculate the footprint and rooftop area.

The results of these calculations use the average efficiency range of 15%-20% efficiency for mono-crystalline photovoltaics (NREL, 2020), solar roof arrays covering 80% of the available roof area yields 23% to 31% of the building's estimated energy needs based on building area in both locations. To achieve net zero energy status, Ikea Furuset would need between 21,835 sqm and 32,342 sqm, while Ikea Slependen would need 30,272 sqm to 44,838 sqm of additional solar arrays. From the cite's gross area, this is achievable for Ikea Furuset, but not Ikea Slependen to reach with carport solar roofs or similar systems to utilize surrounding areas. Although the Oslo locations have a significantly different climate and likely lower irradiation values than the featured example of combination of solar roof and solar car park coverings in Maryland, these findings show the viability of large-scale solar installations in industrial and retail areas of similar density and configuration.

Chapter 7: Street to Building Height Ratio

This chapter will examine the relationship between surface upon which a vertical solar installation is arranged and the primary shading obstacle to the building's facade in dense urban areas. Many of the strongest contributing factors of the latitude of the location, orientation of the street grid, and time of year, have been covered in greater detail in previous chapters. This examination combines many factors by calculating the altitude angle with the degree of latitude, dependant on a specific time of year on a simplified, orthogonal street layout.

For an example of the dramatic effects of this shading, New York City rapidly became an area of dense high-rise buildings to better house its dense population. When it became evident that these structures were creating streets in near constant shadow, the city instituted zoning laws for tall buildings to be set back from the sidewalk and further step back from the street at certain heights to allow more natural light to directly reach the ground level. In turn, this also created an iconic silhouette for skyscrapers in that area. In such cases, potential application of vertical solar installations can be impeded more by the configuration of surrounding buildings than the limitations building containing the installation.

Determining a street's necessary width primarily pertains to the expected travel volume, but once established, there are a variety of functions that can occupy these urban corridors. From pedestrian streets to multi-lane streets of commuter vehicles, a street's composition can greatly influence how people interact with the buildings along it. Though not the only factor, it is one of the most significant in shaping the experience of the area. Dedicating more space

to vehicles signals a corridor to pass through while wider sidewalks encourage pedestrians to linger. Streets with dedicated spaces for public transit, such as bus, tram, high occupancy vehicle, or bike lanes will promote those types of vehicles. The dedicated lanes may encourage these vehicles to operate at higher efficiency and improved accessibility than if all vehicles shared the same undesignated lane. The diagram below compares the configuration a street with undesignated lanes to one with various types of designated lanes. Both streets are the same overall width, though the example to the right accommodates a greater variety of vehicles.

Figure 24: Lane Designation

Regardless of the variety of functions designated for the street, the overall width is the only relevant factor for vertical solar installations as it represents the distance between the surface with the solar installations and the primary surface projecting shadows upon of it. In dense urban areas of at least mid-rise height, the primary shading structure is likely to be the buildings directly across the street. Depending on the density of high-rise structures, areas of large height differences may cast shadows over several adjacent blocks.

Case Study: Street Shadows in Oslo

For these calculations, the latitude input is the absolute value of the degree from the equator. This means the number is positive, regardless to if the location is north or south of the equator, as locations in the southern hemisphere are sometimes denoted with negative degrees.

To determine the amount of vertical area a surface receives throughout the year, this can be estimated with some degree of accuracy using the extremes of solar angles measured at the summer solstice, the sun's highest point resulting in the solar maximum, and winter solstice, the sun's lowest point resulting in the solar minimum also called the solar constant. Between these two values is the angle determined by the solar equinox, the vernal (spring) and autumnal (fall/autumn), which result in the solar average.

Using the solar constant results in the height of the façade that will be the minimum value that is in sunlight throughout the year. This value is very helpful for solar installations, showing how much of the top of the façade is in most constant sunlight, though this value is likely to be small compared to the total available area. The solar maximum conveys only the height at the peak of sun exposure, which is impractical for determining the extent of solar installations but may convey some other importance. What may be the most practical is that of the equinox, resulting in an average value, as solar installations up to this height will be in sunlight for half of the year. Between the vernal and autumnal equinox, the façade will, at minimum, have consistent sunlight up to the projected height.

Once the appropriate solar angle is established, three other measurements can be combined to determine the amount of solar coverage:

the height of the two buildings and the distance between them. As this example is an area of consistent height, the most relevant shading object for the given building is the building directly across the street. The following equation shows how these values are determined using the measurement for the equinox, although the variables can be substituted in using the variables from the variables table.

$$(W_s \times \tan(E_e)) + (h_d) = h_e$$

(Street Width x Tan(90-Latitude)) + (Solar Surface - Shading Building Height) = Average Solar Height at Equinoxes (measured from the top of the building)

This same equation can be used to solve for any individual variable depending on which may have been determined by other factors. Solving for street width can be applied in the planning of new developments to achieve a specific amount of vertical solar façade. Alternatively, in urban areas where the street width is established, these calculations can provide guideline for prospective building alterations with the intention of improving vertical solar potential.

For these calculations, azimuth is measured facing the equator, casting values in the counter clockwise direction as negative and positive values in the clockwise direction. For the purpose of clarity, as this case study is in the northern hemisphere, southeast faces would be negative up to the maximum value of -90° due east and southwest would be positive values to the maximum value of 90° due west. As discussed in chapter 4, the rotation of a street's grid can greatly impact the amount of direct sun exposure a vertical surface

achieves. To simplify this variable, the example pair of buildings in the following shading diagrams are oriented due north and south of a street which runs directly east to west, which sets the street azimuth at 0° for the purpose of this set of examples. The building on the northern side of the street and left side of the figures is south facing, henceforth called ‘Building A’. The opposite building, henceforth called ‘Building B’, is on the south side of the street and corresponding to the right side of the figures. Building B casts a shadow on Building A, given that this example is in the northern hemisphere and uses the solar angles measured for the Oslo at a latitude of 59.9139° N.

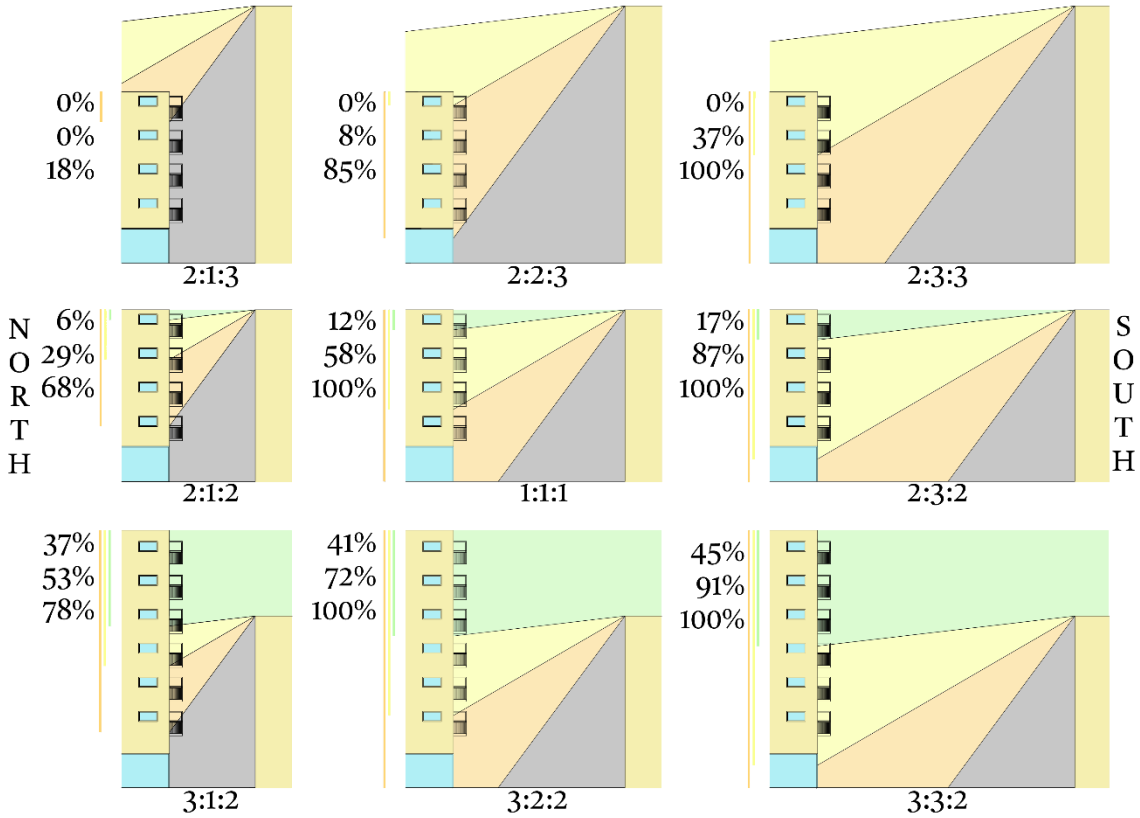

Figure 25: Matrix of Shading Ratios

Examining the same configuration in section, the diagram showcases buildings varying heights and the street between at varying width. The measurements can be simplified into a ratio to apply the findings to areas with similar proportions. Although it is well known that wider streets allow more

natural light to reach street level, this helps to quantify to what extent that distance can affect the vertical solar installations.

The columns from left to right use examples with progressively wider streets. Also, the rows from top to bottom range from examples where Building B is taller than Building A, both are equal or approximately equal heights, and Building A is taller than Building B. The colors in the intermittent space represent as a line of shading as follows: green for the area that will be in direct sunlight throughout the year even at the sun's lowest point on the winter solstice, yellow for the area in sunlight from the winter solstice to either equinox, orange for the area in direct sunlight from either equinox to the sun's highest point on the summer solstice, and grey for the area that does not receive direct sunlight at any point of the year. Obviously, installations in the green area are the best for solar applications with descending suitability approaching street level. However, as the diagram shows, this is not always possible, depending on the ratio.

The following diagrams again use the latitude for Oslo to calculate these shadows and proportions in buildings of equal or near equal height. These ratios are based on nearest whole numbers for areas of mid-rise height. The first shows a configuration that will achieve a minimum of half of the building façade in full sunlight for half of the year, a ratio of 10:9:10, compared to the second configuration, a ratio of 4:7:4, for the entire façade to be in sunlight for half of the year.

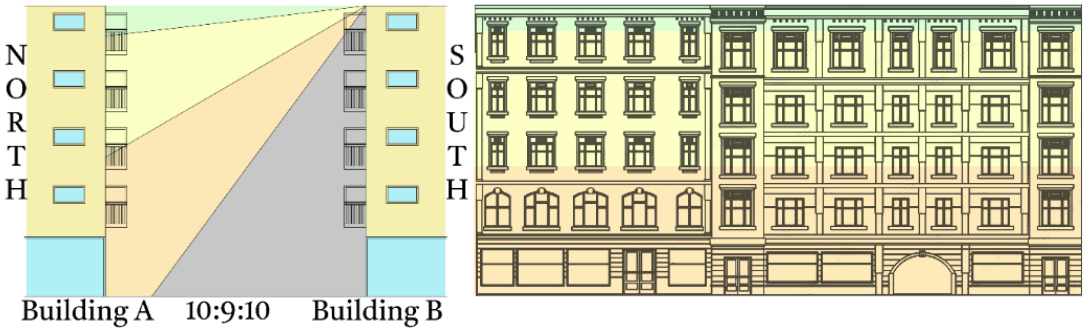

Figure 26: Oslo 50% Direct Radiation

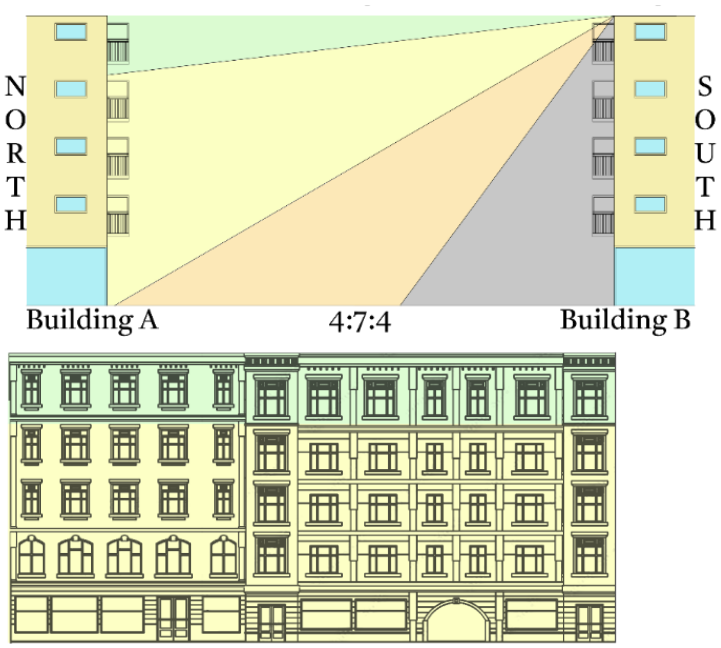

Figure 27: Oslo 100% Direct Radiation

Chapter 8: Oslo Case Study

This chapter focuses on hypothetical calculations for solar potential in three areas of Oslo with different densities. Each takes into account the lengths of the blocks facing a south direction, average heights of the buildings, the average amount of the vertical surface in sunlight, and the amount of an area available for installations. The value of efficiency for roof and vertical façade panels is between 15%-20% efficiency for mono-crystalline photovoltaics (NREL, 2020) and the efficiency transparent window solar is 7% (How It Works - ClearVue PV, 2022). The projected end value of energy from these installations is measured in megawatt hours. Observed areas are outlined in red in the map bellow, with building footprints shown as filled black shapes with the ground in light grey to contrast the waterfront shown with darker grey.

Figure 28: Oslo Figure Ground Map

Using the building footprints from the program QGIS, the target buildings are broken into the southeast and southwest facing sides, the lengths of which

are individually totalled. The building height component is a more complicated value to estimate, even by average. In this case, the solar radiation values used are from the PVGIS system used in previous chapters (JRC Photovoltaic Geographical Information System (PVGIS) - European Commission, 2016).

Next, using the method described in the chapter on building to street width ratio yields an approximate shading value based on the surrounding structures. The area of Oslo Sentrum is a combination of somewhat consistent street widths and block heights has somewhat consistent shading. The collection of buildings measured at Sørenga is on a peninsula jutting into the harbour with one, wide road running through the middle of the building area with little surrounding shading. Barcode is a group of high-rise buildings facing a broad street along its southwest side, which leaves much of the surface unshaded throughout the year. The following diagrams show an examination of these areas and the corresponding building to street ratio of each. Of the three areas, the one in the city center has the most surrounding shading. Only the height in full sunlight measured from the top of the façade on the equinox is recommended to maximize the return on investment.

Another relevant factor is how much of each surface area is available for solar installations. Many roof areas are dedicated to private terraces of adjacent apartments or areas of vegetation and must be removed from consideration for rooftop solar. The potential area of vertical surfaces is reduced by an estimated percentage based on how much of the surface is windows or contains features that solar arrays would have to be installed around or on top of. For all of the case studies, 70% of the vertical façade in sunlight on the equinoxes is dedicated to solar installations and 80% of the available roof area. The

estimation is broken up to approximate what amount of the façade is composed of windows while leaving 30% of the available area to account for spacing between the panels and features of the building, such as drainage pipes or flashing, that these panels would have to be installed around.

Finally, comparing the projected solar energy generation to how the energy demand of the same area shows the potential benefit of such applications. The European Union annual specific energy consumption for all types of building was around 215 kWh/m^2 in 2016, which can be subdivided into 300 kWh/m^2 for commercial buildings and 178 kWh/m^2 for residential (*Progress on Energy Efficiency in Europe*, n.d.). According to *Statistisk Sentralbyrå* (*Energy consumption in households, 2012*, 2014) the average energy consumption in Norwegian households is 149 kwh/m^2 as of 2012. The case study areas are all mixed use, with commercial areas occupying the lower floor or floors of a building with residential areas above. To provide a more accurate estimation, the European Union value for commercial areas is used for the first floor and the value for Norwegian residential consumption for all floors above. Applying the value for Norwegian households alone would be an underestimation, as it would not include increased demand for commercial areas. The building footprints multiplied by the average number of stories yields an estimated building area. The estimated building area multiplied by the energy consumption yields an estimated energy demand for the cite. The projected production from the solar installations can then be expressed as a percentage of the estimated electricity demand for the cite.

((Total Building Footprint Area (m^2) × EU Commercial Energy Consumption (300kwh/m^2)) + (Average Number of Stories above 1st × Norway Residential Energy Consumption (149kwh/m^2) = Estimated Energy Demand (kwh)

(Estimated Solar Production ÷ Estimated Energy Demand) × 100

= Percent of Energy Provided by Solar

Summary Answer: Although these areas were not designed to accommodate large solar installations, these can contribute greatly to the energy demand by optimizing the surrounding building morphology.

Area 1: Oslo Sentrum, does not include roof solar due to limitations in measurement. The resulting estimation between 33,109 m^2 and 40,743 m^2 of solar panels will generate between 3,224MWh to 5,219MWh of electricity. This is between 1.33% and 2.16% of the estimated energy demand.

Area 2: Sørenga, the highest yield result, has the best direction and spacing. The estimated range goes from 54,398m^2 to 58,946m^2 of solar panels generates a projected 6,104 MWh to 8,365 MWh of electricity, which should serve between 8.37% and 11.47% of the estimated energy demand.

Area 3: Barcode only uses the short face of the building, which has the most optimal solar direction. With little surrounding shading, 37,256m^2 of solar panels yields between 5,630MWh and 7,412MWh of electricity, or between 4.25% and 5.82% of the estimated energy demand due to the efficiency range.

Area 1: Oslo Sentrum

Area 1 is a mid-rise area in the historic central district of Oslo, from which the area is called *Sentrum*, meaning downtown. The area examined totals twelve city blocks taking up over forty-four hectares. Spacing between the

buildings ranges from around 10m to 14m and the average height measured from thirty-six different points is approximately 19.55 meters (h_t) taken at the south, southeast, and southwest corners of each block of buildings.

Characteristically of an area with significant historic value, preservation of historic facades and materials present impediments to vertical solar installations. This area is a prominent shopping district, hosting pedestrian foot traffic as well as its location adjacent to many connection points of public transportation. There is likely to be strong resistance to changing these historic facades, however, should this be accomplished, it could serve to normalize the type of installation in other areas of the city. The roofs in this area are combinations of gabled and hipped roofs of varying slopes. As the slope and direction of the roofs in this location varies so much, the roof area is excluded from a potential solar installation, although it can be effectively placed on a more individual basis.

The lower end of the boundary is determined using the minimum average efficiency of 15% for standard panels and that vertical installations are located only above the point of the solar average. Solar average here is measured as the top portion of the average building height using the elevation angle of the sun on the equinox and a given value for street width. In contrast, the upper boundary for these estimations uses the higher average efficiency of 20% for standard panels and that vertical installations are located along the entire average potential height or the average height of the area except for 4 meters at street level. This process yields a range from utilizing the most optimal solar areas based on the urban configuration at the lower end to the

maximum that could be expected to be produced in the same configuration at the upper end.

Table 8: Oslo Sentrum Calculations

Mid-Rise (hp > 8 stories or 32m)		Oslo		Sentrum	
Borders:	Rådhusgata	Skippergata	Karl Johans gt.	Nedre Slottsgate	
Flat Roof Irradiation with Optimized Slope and Azimuth (kwh/m2)			1152.29	Sun Angle at Equinox (E_e)	30.09
SW Azimuth (0 to 90)	25	SW Solar Irradiation (kwh/m2)	876.69	Cite Gross Area (m2)	443,211
SE Azimuth (0 to -90)	-65	SE Solar Irradiation (kwh/m2)	722.22	Building Footprint Area	275,096
Stories (Average):	5	Available Roof Area	0	FAR Calculation (Density)	3.03
Average Building Height (hp)	19.55	Negate First Floor (hs)	4m	Adjusted Average Height	15.55
Shading Building Height	19.55	Street Width (m)	13	Ratio	20:13:20
Average Building Area (m2)	1,344,823	EU or Norway Avg. kwh/sqm	300 or 149	Avg. Building Mwh Use	241,918
Reccomended Based on Shading (15% efficency panels, 7% efficency glazing, solar average height)					
SW Solar Average (m)	8.56	44%	SE Solar Average (m)	15.55	80%
Total SW Length (m)	1559	Calculating Vertical Area		Total SE Length (m)	2183
Total Vertical Area (m2)	47,299	SW Area Potential (m2)	13,344	SE Area Potential (m2)	33,955
Facade Standard Panels		Facade Window Solar		Percent Roof Panels	
Percent of Facade	50%	Percent of Facade	20%	Percent of Roof	0%
Adjusted Area (m2)	23,650	Adjusted Area (m2)	9,460	Adjusted Area (m2)	-
Kwh	2,716,629	Kwh	507,104	Kwh	-
Total Solar Kwh	3,223,733	Total Solar Mwh	3,224	Percent Solar Energy	1.33%
Maximim Potential (20% efficency panels, 7% efficency glazing, adjusted average height)					
Facade Standard Panels		Facade Window Solar		Percent Roof Panels	
Percent of Facade	50%	Percent of Facade	20%	Percent of Roof	80%
Adjusted Area (m2)	103,780	Adjusted Area (m2)	41,512	Adjusted Area (m2)	0
Kwh	4,578,179	Kwh	640,945	Kwh	-
Total Solar Kwh	5,219,124	Total Solar Mwh	5,219	Percent Solar Energy	2.16%

This case study yields the lowest energy return, due in part to the lack of roof solar. The lower end of the estimation finds that 33,109m^2 of solar panels generating 3,224 MWh or 1.33% of the estimated energy demand of this area of the city. Conversely, the maximum projected result in this system of 40,743 m^2 of solar panels generating 5,219 MWh of electricity or 2.16% of the area's estimated energy demand. Many roofs in this area suitable for solar installations, however, they cannot be consistently measured to an accurate degree with the tools of this examination. Despite this difference, using exclusively vertical solar mounting can still offset a significant energy demand.

Area 2: Oslo Sørenga

Area 2 is a mid-rise area spanning over thirty hectares, as many of the buildings were completed in r while other adjacent lots are still under construction as of the writing of this thesis. The area slopes significantly with some areas that access different stories of the same building at ground level. Spacing between the buildings ranges from 34m on the main road to around 11m for the auxiliary roads. The average height measured from sixty-nine different points is approximately 18.09 meters (h_t) as many buildings are subdivided into terraces of different heights. The perimeter of the area serves as a generous pedestrian circulation with a dock for swimming and lounging at the end of the peninsula.

The location upon a peninsula yields that over half of the buildings face an unshaded waterfront along a side that is somewhat south oriented, which allows for a street to building height ratio using the central road width and average building height of 9:17:9 with 79% of the façade in sunlight on the equinox. Its configuration is such that two rows of blocks are separated by a central road with perpendicular arteries. For this reason, a separate ratio is used for the smaller streets facing southwest with a building to street ratio of 18:11:18 with 53% of the façade in sunlight on the equinox as the buildings are closer together.

Table 9: Oslo Sørenga Calculations

Mid-Rise (hp > 8 stories or 32m)		Oslo		Sørenga	
Borders:	Bjørvika peninsula south east of the intersection of Sørengkaia and Rostockgata				
Flat Roof Irradiation with Optimized Slope and Azimuth (kwh/m2)			1152.29	Sun Angle at Equinox (E_e)	30.09
SW Azimuth (0 to 90)	48	Solar Irradiation (kwh/m2)	808.14	**Cite Gross Area (m2)**	303,584
SE Azimuth (0 to -90)	-42	Solar Irradiation (kwh/m2)	798.51	**Building Footprint Area**	88,459
Stories (Average):	5	**Available Roof Area**	31,650	**FAR Calculation (Density)**	1.32
Average Building Height (hp)	18.09	**Negate First Floor (hs)**	4m	**Adjusted Average Height**	14.23
Shading Building Height	18.09	**SE Street Width (m)**	34	**SE Ratio**	9:17:9
Average Building Area (m2)	399,991	**EU or Norway Avg. kwh/sqm**	300 or 149	**Avg. Building Mwh Use**	72,956
Reccomended Based on Shading (15% efficency panels, 7% efficency glazing, solar average height)					
Solar Average (m) SW	9.52	53%	Solar Average (m) SE	14.23	79%
		SW Street Width (m)	11	**SW Ratio**	18:11:18
Total SW Length (m)	730	Calculating Vertical Area		Total SE Length (m)	1214
Total Vertical Area (m2)	24,231	SW Area Potential (m2)	6,953	SE Area Potential (m2)	17,279
Facade Standard Panels		Facade Window Solar		Percent Roof Panels	
Percent of Facade	50%	Percent of Facade	20%	Percent of Roof	80%
Adjusted Area (m2)	24,231	Adjusted Area (m2)	4,846	Adjusted Area (m2)	25,320
Kwh	1,456,199	Kwh	271,824	Kwh	4,376,397
Total Solar Kwh	6,104,420	**Total Solar Mwh**	6,104	**Percent Solar Energy**	8.37%
Maximim Potential (20% efficency panels, 7% efficency glazing, adjusted average height)					
Facade Standard Panels		Facade Window Solar		Percent Roof Panels	
Percent of Facade	50%	Percent of Facade	20%	Percent of Roof	80%
Adjusted Area (m2)	13,834	Adjusted Area (m2)	19,791	Adjusted Area (m2)	25,320
Kwh	2,219,388	Kwh	310,714	Kwh	5,835,197
Total Solar Kwh	8,365,299	**Total Solar Mwh**	8,365	**Percent Solar Energy**	11.47%

Of the three areas, this region of Sørenga yields the highest solar energy for this configuration. At the lower end of the range, 54,398m^2 of solar panels generating a projected 6,104 MWh of electricity, which should serve 8.37% of the estimated energy demand. Conversely, at the upper end of the range, an installation of 58,946m^2 of solar panels generating a projected 8,365 MWh of electricity, which should serve 11.47% of the estimated energy demand. Many portions of the roof are dedicated to terraces and balconies, but a significant portion remains available for solar installations. This combination of vertical wall, window, and roof solar in a mid-rise area with little surrounding shading culminates in a substantial contribution of renewable energy.

Area 3: Oslo Barcode

Area 3 is an unusual area of Oslo, totalling just under twenty hectares. a row of unique, artistically designed high rise buildings. The north of these buildings face the tracks running to the central train station, displaying to travellers the barcode like appearance for which this area is named. In contrast, the south faces an unusually wide street with buildings of consistent mid-rise height across the street. These rectangular buildings are oriented with the short sides of the building footprint facing the wide street along the southwest side, while the longer sides of the buildings are separated by streets of around 7m to 11m in width. With this arrangement, the longer sides of the building are largely in shadow, while the short sides are in nearly constant sunlight. For this reason, only the southwest side, the shorter face of the rectangular buildings is used for calculations for potential solar installations.

As this example area has significant height differences between the shading structures from the surface of proposed solar installations, the resulting ratio is 29:45:37. Likewise due to the wide street adjacent to the façade with solar installations, the entire façade is in direct sunlight on the equinoxes. As a result, the total area of solar installations is the same between the two examples and the difference in efficiency is the only changed variable in the range of resulting electricity generation. These buildings vary in levels of glazing, ranging to one building with a fully glazed façade. For this reason, the percentage of glazed solar is higher than in other case studies.

Table 10: Oslo Barcode Calculations

High-Rise (hp > 8 stories or 32m)		Oslo		Barcode	
Borders:	Rv 162	Dronning Eufemias gate	Trelastgata	Nylandsveien	
Flat Roof Irradiation with Optimized Slope and Azimuth (kwh/m2)			1152.29	Sun Angle at Equinox (E_e)	30.09
SW Azimuth (0 to 90)	27	Solar Irradiation (kwh/m2)	858.34	**Cite Gross Area (m2)**	198,350
SE Azimuth (0 to -90)	-63	Solar Irradiation (kwh/m2)	718.75	**Building Footprint Area**	71,135
Stories (Average):	11	**Available Roof Area (m2)**	32,806	**FAR Calculation (Density)**	3.95
Average Building Height (hp)	44.02	**Negate First Floor (hs)**	4m	**Adjusted Average Height**	40.02
Shading Building Height	28.70	**Street Width (m)**	45	**Ratio**	29:45:44
Average Building Area (m2)	782,922	**EU or Norway Avg. kwh/sqm**	300 or 149	**Avg. Building Mwh Use**	127,397
Reccomended Based on Shading (15% efficency panels, 7% efficency glazing, solar average height)					
SW Solar Average (m)	40.02	91%	SE Solar Average (m)	-	-
Total SW Length (m)	393	Calculating Vertical Area		Total SE Length (m)	0
Total Vertical Area (m2)	15,730	SW Area Potential (m2)	15,730	SE Area Potential (m2)	-
Facade Standard Panels		Facade Window Solar		Percent Roof Panels	
Percent of Facade	40%	Percent of Facade	30%	Percent of Roof	80%
Adjusted Area (m2)	6,292	Adjusted Area (m2)	4,719	Adjusted Area (m2)	26,245
Kwh	810,084	Kwh	283,529	Kwh	4,536,243
Total Solar Kwh	5,629,856	**Total Solar Mwh**	5,630	**Percent Solar Energy**	4.42%
Maximim Potential (20% efficency panels, 7% efficency glazing, adjusted average height)					
Facade Standard Panels		Facade Window Solar		Percent Roof Panels	
Percent of Facade	40%	Percent of Facade	30%	Percent of Roof	80%
Adjusted Area (m2)	6,292	Adjusted Area (m2)	4,719	Adjusted Area (m2)	26,245
Kwh	1,080,112	Kwh	283,529	Kwh	6,048,324
Total Solar Kwh	7,411,965	**Total Solar Mwh**	7,412	**Percent Solar Energy**	5.82%

This scenario is the middle of the three results. The lower range is 37,256m^2 of solar panel installations yielding 5,630MWh of electricity, or 4.42% of the estimated energy needs of the area. At the higher end, 37,256m^2 of solar panel installations yielding 7,412MWh of electricity, or 5.82% of the estimated energy needs of the area. However, it should be noted that of the three scenarios, this is the only of the three only using one face of the buildings for the vertical installations. Likewise, as the only example with high-rise buildings, the estimated building area is relatively high compared to the overall cite area and the energy needs of the building may be higher than estimated depending on the insulation of the large areas of glazing.

Analysis

As Chapter 1 discussed, the overall quantity of solar installations is increasing as well as an expanding variety of potential alternatives that integrate renewable energy generation in dense urban areas. These combined land use solutions encompass a broad range of applications ranging from the agricultural to artistic. Among the possible architectural applications, this thesis examined the applications of vertical panels, solar glazing, and solar arrays on flat roofs. The versatility of solar panels is such that they can be effectively deployed on virtually any building surface.

Numerous policy approaches discussed in Chapter 2 exist to integrate the new solar installations at scales ranging from the individual to groups of countries. Achieving a greater uniformity in implementation across various areas and scales will facilitate their adoption and integration. Furthermore, increasing proliferation of policies with objectives similar to the Energy Performance of Buildings Directive will necessitate the energy use of all new areas to be a consideration for architects and planners. Energy use and production will become more closely attached to the design of the built environment as regulations mandate a movement approaching net zero energy and energy plus buildings. Consequently, thoughtful design of building systems and insulation will become increasingly relevant in reducing energy demand. In accordance with the findings from the case studies of other chapters, it can be concluded that the low efficiency of solar glazing creates the lowest energy return system per square meter. Installations on flat roofs are the most effective, as they can be directed in the optimal direction and slope, though roofs are frequently occupied by roof terraces or sloping roofs. Contrarily, although

lacking in optimal slope and direction, the advantage of vertical solar is that a high quantity of otherwise unoccupied area that can be utilized.

The applicability of this series of calculations stems from two key factors: streets are largely laid out in orthogonal grids and the path of the sun is predictable. Chapter 3 focused on how to apply the latitude of a location. The focus of Chapter 4 applied street rotation, or building azimuth, both on solar radiation potential and projecting shadows that limit direct beam radiation. The result was that street orientations rotated approximately equilaterally, such as that of the Barcelona street grid, have the lower levels of direct sunlight or direct beam radiation, regardless of whether the buildings are arranged in square or rectangular configuration. In contrast, configurations with more disparate angles, in this case, that of the New York City street grid, produced higher surrounding sunlight and direct beam radiation on surrounding surfaces. The difference is slight for square configurations, with a variance of 1.5%, and greater for rectangular configurations, with a variance of 23.9%. Furthermore, Chapter 7 examined the relationship between the height of buildings and the spacing between. To achieve vertical surfaces with minimal shading, areas closer to the equator can have narrow distances in between them while areas closer to the poles require wider streets. This necessitated the development of a set of excel tools to calculate the interaction between changing variables. Combined, a location’s latitude and street orientation effect the amount of direct beam radiation striking the vertical surface with solar installations calculated using the street to building height ratio.

The case studies in Chapter 5 comparing The Empire State Building and the Seagram Building in New York exemplify the difference that the scale of

vertical installations can make, even by utilizing the least efficient option. The Empire State Building case study found that 6,052m^2 yields 415.51MWh of electricity, or an estimated 1.16% of the building's estimated energy usage. By comparison, the case study of the Seagram Building resulted in an estimate that 13,285m^2 of solar glazing will result in a projected 945.51Mwh of electricity, or 2.63% of the building's estimated energy usage. However, the energy demand of each may be higher than estimated, due to aging building systems and lower energy standards at the time of their construction. As the later has double the area, the energy production is therefore doubled. The difference is that The Seagram Building's façade, composed of a majority of glass and framework, leaves no other locations to attach any other vertical solar options while The Empire State Building has fenestrations spaced in a smooth stone facade. This allows the possibility of attaching standard solar panels in vertical arrays of significantly higher efficiency than solar glazing. Despite solar glazing possessing the lowest efficiency of models used in this thesis, this form of solar installation possesses some advantages due to its flexibility.

Chapter 6 showcased a type of structure well suited for rooftop solar capable of supplying 23% to 31% of the estimated energy use of these areas. As established in the description of the area, there is a significant quantity of unoccupied area to extend solar installations to increase energy supply. Conversely, these example areas are low-rise buildings that only makes up a small amount of the gross cite area. This density can be measured by the floor area ratio (FAR) which is a ratio of the gross cite area to the overall building area. For example, these two IKEA locations have a density of 0.56 in the Furuset location and 1.3 in the Slependen location compared to the Oslo case

studies with FAR values of 3.03 for Oslo Sentrum, 3.95 for Oslo Barcode, and, the area with the most similar density, 1.32 for Oslo Sørenga. It must be stated that there is greater room for error in this later value, as the footprints of structures currently under construction in the area are not included. In addition, the building height is measured from the ground level but multiple buildings in the Sørenga case study area have occupied stories below ground level due to sloping terrain. Higher density areas will have a significantly higher energy demand.

Finally, Chapter 8 combined the processes of previous chapters in three case study areas. In addition to the roof and glazing solar options demonstrated in previous chapters, this also added vertical solar installations to the exterior facades. These calculations found two values for the range of solar potential of the areas; the lower range value used the vertical building height determined by the point of direct beam radiation at the equinox using 15% efficiency for the standard panels and the higher end of the range uses the building's potential height (the average height minus 4 meters to exclude the pedestrian way) at 20% efficiency for the standard panels. Area 1 yielded the lowest returns in providing between 1.33% and 2.16% of the estimated energy demand due to the exclusion of rooftop solar. Area 2 yielded the highest returns in providing between 8.37% and 11.47% of the estimated energy demand due to its rotation and spacing. Area 3 yielded a more variable range, providing between 4.42% and 5.82% of the estimated energy needs of the area, although it only used one face of the building compared to the other areas, which used two faces for potential vertical installations.

Conclusion

Based on the examinations throughout this thesis, these findings amount to a collection of recommendations for urban planners to design dense urban areas suitable for solar installations or building integrated photovoltaics (BIPV). To apply the most relevant result for urban planning recommendations are to utilize more efficient passive and active building systems, adjust the street grid and building orientation, optimise the building height to street width ratio, select surfaces for solar installations, and maximize sun facing facades.

Of all of these reccomendations, though of less direct relivance to planners, the improvment building systems, both passive and active, propelled by increasingly environmentally motivated policies can decrease energy demand. The integration of solar water heating systems can fulfill the building's water heating requirements with thermal collectors to capture the natural thermal radiation. Choosing energy-efficient appliances and LED lighting, and smart controls likewise reduce electricity demand. The goal of smart systems is to optimize performance by monitoring energy systems. These should be regularly analyzed to identify potential improvements. Finally, energy storage systems consisting are nessisary to store excess solar energy generated during the day for use during non-sunny periods to ensure greater self-sufficiency, resilience, and consistent power supply for the area. These performance of these building systems will continue to be determined by energy regulations and policies that will gradually lead the transtion to more sustainable building practices.

Depending on the location of the cite, it is possible to optimize the building orientation to reduce shading on vertical solar installations on adjacent structures. Although this is not fasible for retrofitting existing areas at smaller scales, it is applicable for planning new areas and larger scale city planning projects where adjustments including realigning street girds is relivant. Generally, street rotation around 45 degrees from the orthogonal has a higher level of shadows than more dinamic angles within 15 to 20 degree additional rotation in either direction. These findings were that locations within the tropics (23.5 degrees north to 23.5 degrees south of the equator) and some distance beyond that division, street rotation has no impact on shading unless the buildings are very close together. As the latitude of locations approaches the poles, the optimal building azimuth angles between the two surfaces have increasing difference between the two values to minimise shading. For blocks that are rectangularly shaped, the long face of the building should be rotated the corrispondingly larger value and the short face the smaller value. One such example may be that the longer southeast face of a building could be rotated -60 degrees (where the negative denotes the eastward direction) and the shorter building face is rotated the corrisponding 30 degrees in a southwest direction. A specific value or range of optimal values can be found by using the formulas previously explained throughout this thesis. The overall impact of this aspect is slight compared to other features of the urban landscape.

Once the orientation is established, the next step is to take propotionate spacing into account. When designing new buildings, planners and architects should consider the solar path to maximize solar exposure. Building heights are often restricted by local zoning regulations, though, beyond that restriction, this

aspect can be converted to an optimal solar area with thoughtful consideration of the surrounding built context. Intermittent spacing between buildings should be of appropriate size according to the building height to street width ratio to achieve a vertical solar installations in direct beam radiation for larger portions of a year. This is dependant on the latitude of the location as well as the solar altitude ange most relivant to the goals of the project. Ensuring gernerous pedestrian areas can widen transit corridors to avoid excessively shaded street levels, though this should be balanced with the transit needs of the area.

After the general proportion of the building or urban area is determined, the next relivant process is selecting which solar applications should be most emphasized in the design based on the objectives of the project. Eventhough virtually any architectural surface can be transformed into a solar surface, a flat roof or a single sloped roof already optimally oriented for direction and slope have the highest energy return. Vertical mounting and existing roof slopes yeild a lower energy return than the alternative, but limitations on available area for mounting lend to the flexibility of applications. Similarly, solar glazing operates at significntly lower efficency as it allows a portion of the visable light spectrum to pass through. As a result, buildings should emphazixe this type of roof and available area. Colder climates may incorporate passive solar design strategies such as large windows on sun facing sides of the building with solar glazing to increase daylighting and natural heating along with energy generation. Conversly, warmer climates may incorperate sun shading systems to generate electricity while also reducing the solar radiation striking the building’s surface.

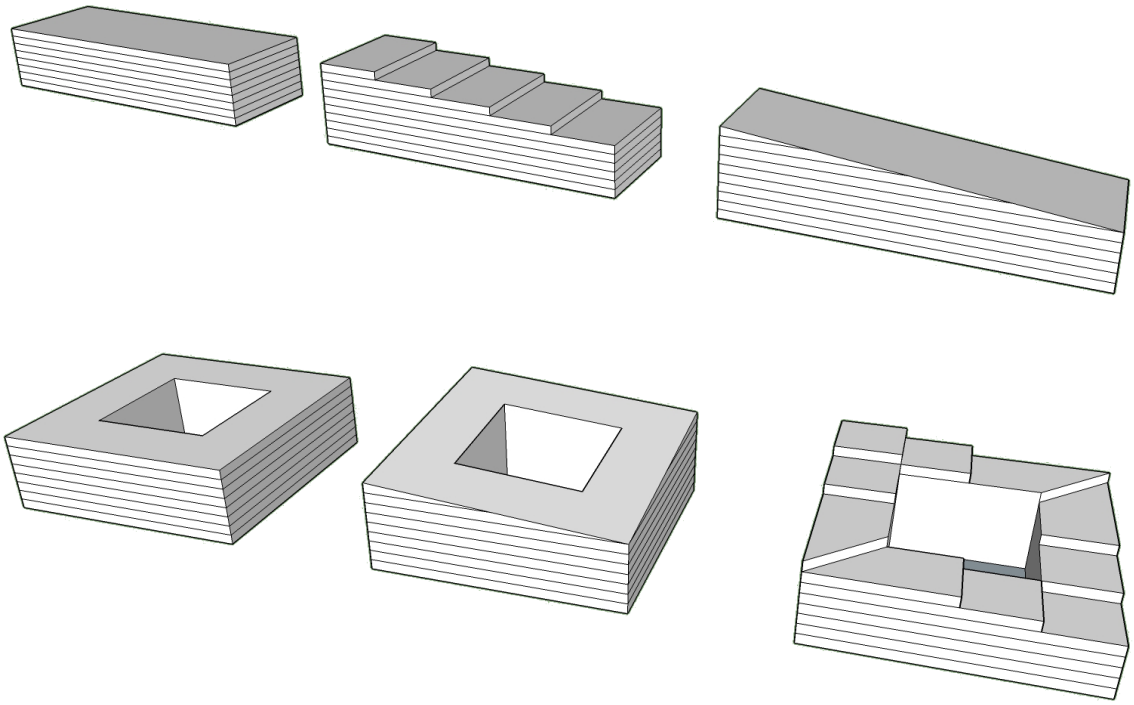

Figure 29: Solar Building Morphologies

Once the relivant solar applications are selected, the next consideration is to maximize solar facing surfaces for the selected features. It should be noted that for locations within the tropics (23.5 degrees north to 23.5 degrees south of the equator), the sun direction has significantly more variation in direction of sun and shadows, making more building faces optimal for solar installations, though limited by time of year. On the equator, shadows point south for half of the year, north for the other half, and only due east and west on the equinoxes. Most of these reccomendations are for locations outside of the tropics, though these can still be applied with slight adjustments. A relevant example outside of the tropics in the northern hemisphere with a focus on vertical solar installations would be taller south facing sides tiered down to shorter north facing sides to reduce shading. Alternatively, another structure in the northern hemisphere with a focus on single slope roof solar would have a taller north face sloping continuously down to the sourh face to maximize continuous roof

area in the optimal direction. These two examples have reversed direction, though both can maximize solar surfaces while reducing surrounding shading if the pattern of the individual structure is repeated in orthogonal blocks. This will contribute to the general shape and overall character of the planned area.

The combination of these design considerations will facilitate the conversion of existing urban areas or designing new areas with a stronger connection to intigrated renewable energy systems. The most significant findings of this thesis are the stratigies to determine the most relivant stratigies depending on the scale, location, and demands of a project. While all but one case study failed to meet the energy needs of the area, this still showed the impact of potential solar installations in each urban context on different building morphologies. Regardless of this, similar solar systems can contribute to the overall goal of net zero energy or energy positve projects in combination with other renewable energy systems and design focused solutions. As architects and planners must increasingly employ sustainable building practices, the flexibility of solar installations shows potential for broad applications in dense urban areas.

References

Al-Kodmany, K. (2014). Green Retrofitting Skyscrapers: A Review. *Buildings*, *4*(4), 683–710. https://doi.org/10.3390/buildings4040683

Boeing, G. (2019). Urban spatial order: street network orientation, configuration, and entropy. *Applied Network Science*, *4*(1). https://doi.org/10.1007/s41109-019-0189-1

Comprehensive Renewable Energy. (2012). Elsevier.

Climatewire, D. D. (2010, August 24). *Making the Big Apple Green Starts with the Empire State Building*. Scientific American. https://www.scientificamerican.com/article/making-big-apple-green/

Dodman, D., B. Hayward, M. Pelling, V. Castan Broto, W. Chow, E. Chu, R. Dawson, L. Khirfan, T. McPhearson, A. Prakash, Y. Zheng, and G. Ziervogel, 2022: Cities, Settlements and Key Infrastructure. In: Climate Change 2022: Impacts, Adaptation, and Vulnerability. Contribution of Working Group II to the Sixth Assessment Report of the Intergovernmental Panel on Climate Change [H.-O. Pörtner, D.C. Roberts, M. Tignor, E.S. Poloczanska, K. Mintenbeck, A. Alegría, M. Craig, S. Langsdorf, S. Löschke, V. Möller, A. Okem, B. Rama (eds.)]. Cambridge University Press, Cambridge, UK and New York, NY, USA, pp. 907-1040, doi:10.1017/9781009325844.008.

Empire State Building -The Skyscraper Center. Retrieved March 27, 2023. https://www.skyscrapercenter.com/building/empire-state-building/261

Energy consumption in households, 2012. (2014, July 14). ssb.no. https://www.ssb.no/en/energi-og-industri/statistikker/husenergi/hvert-3-aar/2014-07-14

Energy Information Administration (EIA)- About the Commercial Buildings Energy Consumption Survey (CBECS). (2016). https://www.eia.gov/consumption/commercial/data/2012/c&e/cfm/pba4.php

Energy performance of buildings directive. (n.d.). Energy. https://energy.ec.europa.eu/topics/energy-efficiency/energy-efficient-buildings/energy-performance-buildings-directive_en

Fraunhofer Institute for Solar Energy Systems. Photovoltaic Report. 2020. (accessed on 1 May 2023). Available online: https://www.ise.fraunhofer.de/content/dam/ise/de/documents/publications/studies/Photovoltaics-Report.pdf

Gholami, H., Røstvik, H. N., & Steemers, K. (2021). The Contribution of Building-Integrated Photovoltaics (BIPV) to the Concept of Nearly Zero-Energy Cities in Europe: Potential and Challenges Ahead. *Energies*, *14*(19), 6015. https://doi.org/10.3390/en14196015

How it works - ClearVue PV. (2022, May 30). ClearVue PV. https://www.clearvuepv.com/products/how-it-works/

IKEA US opens its first solar car park in Baltimore. (n.d.). IKEA. https://www.ikea.com/us/en/newsroom/corporate-news/ikea-retail-u-s-opens-its-first-solar-car-park-in-baltimore-announces-plans-for-seven-more-pub020bd9b7

IPCC, 2022: Summary for Policymakers [H.-O. Pörtner, D.C. Roberts, E.S. Poloczanska, K. Mintenbeck, M. Tignor, A. Alegría, M. Craig, S. Langsdorf, S. Löschke, V. Möller, A. Okem (eds.)]. In: Climate Change 2022: Impacts, Adaptation, and Vulnerability. Contribution of Working

Group II to the Sixth Assessment Report of the Intergovernmental Panel on Climate Change [H.-O. Pörtner, D.C. Roberts, M. Tignor, E.S. Poloczanska, K. Mintenbeck, A. Alegría, M. Craig, S. Langsdorf, S. Löschke, V. Möller, A. Okem, B. Rama (eds.)]. Cambridge University Press, Cambridge, UK and New York, NY, USA, pp. 3-33, doi:10.1017/9781009325844.001.

JRC Photovoltaic Geographical Information System (PVGIS) - European Commission. (2016, January 11). https://re.jrc.ec.europa.eu/pvg_tools/en/tools.html#api_5.2

Progress on energy efficiency in Europe. (n.d.). European Environment Agency. https://www.eea.europa.eu/data-and-maps/indicators/progress-on-energy-efficiency-in-europe-3/assessment

Seagram Building - Data, Photos & Plans - WikiArquitectura. (2020, September 29). WikiArquitectura. https://en.wikiarquitectura.com/building/seagram-building/

Solar Futures Study. (n.d.). Energy.gov. https://www.energy.gov/eere/solar/solar-futures-study

Ubiquitous Energy. (2023, March 1). Ubiquitous Energy. https://ubiquitous.energy/example-installations/

Urban Energy | UN-Habitat. (n.d.). https://unhabitat.org/topic/urban-energy#:~:text=To%20run%20their%20activities%2C%20cities%20require%20an%20uninterrupted,indirect%20emissions%20generated%20by%20urban%20inhabitants%20are%20included.

U.S. Cities Factsheet. (n.d.). Center for Sustainable Systems. https://css.umich.edu/publications/factsheets/built-environment/us-cities-factsheet

Appendices

Figures

Figure 14: Gholami, H., Røstvik, H. N., & Steemers, K. (2021). The Contribution of Building-Integrated Photovoltaics (BIPV) to the Concept of Nearly Zero-Energy Cities in Europe: Potential and Challenges Ahead. Energies, 14(19), 6015. https://doi.org/10.3390/en14196015

Figure 15: Annual changes in the sun's position in the sky (northern hemisphere) *Comprehensive Renewable Energy*. (2012). Elsevier.

Figure 16: Yearly variation of solar declination angle “”

Figure 17: Apparent daily path of the sun across the sky from sunrise to sunset “”

Figure 18: Equinox angles by latitude, own diagram.

Figure 19: *Square-Mile Street Network Visualization*. (2020, October 28). Geoff Boeing. https://geoffboeing.com/2017/01/square-mile-street-network-visualization/

Figure 20: City Street Network Orientation of 100 World Cities. Boeing, G. (2019). Urban spatial order: street network orientation, configuration, and entropy. *Applied Network Science*, *4*(1). https://doi.org/10.1007/s41109-019-0189-1

Figure 21: Street rotation of two cities. Initial image from google maps, overlays added in photoshop. Google Map (2023). [Barcelona, Spain and Manhattan, New York, USA] [Satellite Map]. Retrieved April 15th, 2023.

Figure 22: *Urban Energy | UN-Habitat*. (n.d.). https://unhabitat.org/topic/urban-energy#:~:text=To%20run%20their%20activities%2C%20cities%20require%20an%20uninterrupted,indirect%20emissions%20generated%20by%20urban%20inhabitants%20are%20included.

Figure 23: *Ludwig Mies van der Rohe, Iñaki Bergera · Seagram Building*. (n.d.). Divisare.

https://divisare.com/projects/382675-ludwig-mies-van-der-rohe-inaki-bergera-seagram-building

Figure 24: *Lane Width* | *National Association of City Transportation Officials*. (2015, July 24). National Association of City Transportation Officials. https://nacto.org/publication/urban-street-design-guide/street-design-elements/lane-width/

Figure 25: Matrix of Shading Ratios, own diagram.

Figure 26: Oslo 50% Direct Radiation, own diagram.

Figure 27: Oslo 100% Direct Radiation, own diagram.

Figure 28: Oslo Figure Ground Map. Base map from QGIS using building footprints from the plugin “Open Street Maps” with scale bar and red outline areas added in photoshop.

Figure 29: Solar Building Morphologies, own diagram.

Tables